제 2 형 당뇨병 비약물 치료를 위한

십이지장 점막 재생술 전임상 평가

Preclinical evaluation of duodenal mucosal regeneration for

non-pharmacological intervention of type 2 diabetes mellitus

울 산 대 학 교 대 학 원

의 과 학 과

권 진 희

제 2 형 당뇨병 비약물 치료를 위한
십이지장 점막 재생술 전임상 평가

지 도 교 수   박 도 현

이 논문을 공학박사 학위 논문으로 제출함

2024 년 8 월

울 산 대 학 교 대 학 원
의 과 학 과
권 진 희

권진희의 공학박사 학위 논문을 인준함

심사위원　　박 도 현　(인)

심사위원　　정 진 용　(인)

심사위원　　심 주 현　(인)

심사위원　　민 세 희　(인)

심사위원　　주 지 호　(인)

울 산 대 학 교 대 학 원

2024 년 8 월

감사의 글

저의 학위 과정을 돌아보면 즐거움과 고단함, 얻은 것과 잃은 것, 그리고 도전과 실패의 순간들이 늘 공존하였다고 생각합니다. 그 균형의 순간들을 통해, 모든 것이 당연하지 않다는 것과 그 당연하지 않은 것들에 대한 감사함을 배울 수 있었습니다. 미흡하지만 졸업 논문을 마무리하기까지의 모든 과정들이 결코 혼자서 해낸 것이 아니었기에, 이 감사의 글을 빌려 그동안 함께해 주신 모든 분들에게 감사한 마음을 전하고자 합니다.

먼저 저에게 연구를 바라보는 관점의 확장성을 심어 주시고, 부족한 모습에도 옳은 방향으로 나아갈 수 있게 격려해주신 박도현 지도 교수님께 진심으로 감사드립니다. 저의 엉뚱한 고찰에도 항상 함께 고민해주시고 늘 따뜻한 조언과 지도를 아낌없이 주신 민세희 교수님, 교수님의 조언이 저의 학위 과정에서 큰 위로가 되었습니다. 교수님과 함께 연구할 수 있어 정말 영광이었습니다. 공학적인 관점으로 중개연구를 보완할 수 있는 힘을 실어주시고, 공학도의 귀감이 되어 주신 주지호 박사님께 정말 감사합니다. 비전공자인 저에게 기초의학 배경과 의과학적 학문 지식 성장에 아낌없이 조언해주신 정진용 교수님께도 감사드립니다. 그리고 저의 학위 심사를 위하여 귀한 시간을 내주시어 훌륭하고 날카로운 조언으로 연구의 방향을 지도해주신 심주현 교수님께 진심으로 감사드립니다.

학위 과정 동안 함께 연구에 힘써 주시고 부족한 저에게 빈틈없이 도움을 주던 연구실 동료 김다정 선생님, 배현경 선생님, 김은하 선생님, 이현경 선생님, 김소희 선생님, 임하종 선생님께도 정말 감사드립니다. 그리고 동물 실험 수행에 있어 전문적인 지식과 기술 지원으로 연구를 도와주셨던 김강현 수의사 선생님과 김광훈 선생님께도 진심으로 감사드립니다.

마지막으로 언제나 저를 믿어 주시고 묵묵히 응원해주신 부모님께 감사드립니다. 아버지 어머니께서 삶으로 보여주신 현명함과 지혜로움이 저에게 큰 본보기가 되어, 바르게 성장하기 위해 부단히 성찰하고 노력할 수 있었습니다. 그리고 우리 가족의 활력소 조카 도윤, 새언니, 오빠와 함께한 다채롭고 즐거운 추억들이 고단하던 저의 학위 과정에 큰 위로가 되었고 큰 힘이 되었습니다. 다시 한번 우리 가족들에게 사랑하는 마음을 담아 감사를 전합니다.

이외에도 여기에 미처 적지 못한 많은 분들께 감사드립니다. 저의 순간을 소중하게 만들어준 여러분이 있어 늘 새로운 힘을 얻어 연구에 정진할 수 있었습니다. 진심을 다해 정말 감사합니다.

2024 년 7 월 11 일

권진희 올림

Contents

울산대학교
UNIVERSITY OF ULSAN

Abstract

1. Introduction

Type 2 Diabetes Mellitus (T2DM) have become a major global health concern due to growing adoption of western dietary habits and an increasing aging population. Despite the growing demand for effective treatments, Type 2 diabetes remission using pharmacological methods alone remains challenging. The duodenum has been presented as a key organ for treatment of metabolic disorders including T2DM and obesity. Therefore, it is imperative that innovative non-pharmacological treatments related to the duodenum continue to be developed. Duodenal mucosal regeneration (DMR), which targets thickened mucosa to ablate and regenerate healthy tissue, has recently been implemented. However, current DMR procedures are complex and pose risks of irreversible damage, highlighting the need for developing safer and more effective methods. The aim of this study is to evaluate the therapeutic effects of advanced DMR application using T2DM animal model including rodent and pig. We also assess the efficacy of DMR using application with light emitting diodes (LED)/Organic light emitting diode (OLED) by quantitatively analyzing molecular biological results and gut microbiome changes between the treatment and control groups.

2. Methods & Materials

In this preclinical trial, we utilized Goto-Kakizaki (GK) rat models of T2DM to conduct DMR using endoscopic application with LED/OLED. The study evaluated the safety and efficacy of an endoscopic application equipped with a dual-wavelength (630/850nm) point light source LED module and a catheter with a single-wavelength (650nm) surface light source OLED module. Additionally, scaled-up DMR application which is attachable to endoscopic to assess the potential for clinical application, the safety and efficacy of an expanded endoscopic attachment device with a dual-wavelength LED module were evaluated using T2DM mini pig model. Oral glucose tolerance tests (OGTT) were conducted in GK rats and diabetic mini pigs after fasting overnight to assess blood glucose levels at multiple intervals post-DMR. Biochemical and hormonal analyses were performed on plasma samples to measure liver enzyme activities and hormone concentrations, including insulin, glucagon-like peptide 1, and gastric inhibitory polypeptide. Histological examinations of the duodenum, liver, and pancreas

included Hematoxylin and eosin, Masson trichrome, and multiplex immunohistochemistry staining, followed by digital analysis to evaluate tissue alterations and islet cell morphology. Additionally, microbiome analysis was performed on fecal samples to assess alterations in bacterial composition following DMR.

3. Results

The promising therapeutic outcomes of DMR using LED and OLED catheters highlight the potential of these technologies in treating T2DM and related complications. Our research evaluated the efficacy of DMR with red or infrared LED light in a T2DM animal model, showing significant improvements in serum glucose levels, insulin sensitivity with preserved pancreatic islet and hepatic parameters in GK rats. Similarly, DMR with an OLED catheter resulted in notable reductions in blood glucose levels and improved insulin sensitivity, indicated by lower homeostasis model assessment-insulin resistance levels. Additionally, DMR with LED/OLED light significantly decreased liver fibrosis and altered the gut microbiome. These findings suggest that DMR using LED/OLED catheters directly impacts the duodenal mucosa, leading to consistent metabolic improvements and reduced liver fibrosis, further supporting its potential in enhancing metabolic outcomes.

4. Conclusion

In conclusion, the endoscopic DMR using LED/OLED applications presents a noninvasive approach to improve glycemic control, reduce insulin resistance, preserve pancreatic islet regeneration, and modulate the gut microbiome. The findings not only suggest that DMR could serve as an effective treatment modality for metabolic disorders, including T2DM but also help validate the efficacy and safety of this DMR application. Further clinical trial using the endoscopic attachable DMR application based on dual wavelength are necessary to support the potential of this novel non-pharmacological treatment.

List of Figures

List of Tables

Abbreviation

type 1 diabetes mellitus (T1DM)

type 2 diabetes mellitus (T2DM)

international diabetes federation (IDF)

sodium-glucose cotransporter-2 (SGLT-2)

glucagon-like peptide-1 (GLP-1)

glucagon-like peptide-1 receptor agonist (GLP-1 RA)

gastric inhibitory polypeptide (GIP)

Roux-en-Y gastric bypass (RYGB)

duodenal mucosal regeneration (DMR)

photobiomodulation (PBM)

low-level laser therapy (LLLT)

light Emitting Diode (LED)

organic Light-Emitting Diode (OLED)

Goto Kakizaki (GK)

radiofrequency ablation (RFA)

oral glucose tolerance test (OGTT)

high fat high sucrose (HFHS)

streptozotocin (STZ)

aspartate aminotransferase (AST)

alanine aminotransferase (ALT)

alkaline phosphatase (ALP)

enzyme-linked immunoassay (ELISA)

hematoxylin and eosin (H&E)

Masson trichrome (MT)

Immunohistochemistry (IHC)

interquartile range (IQR)

area under curve (AUC)

homeostasis model assessment-insulin resistance (HOMA-IR)

non-alcoholic fatty liver disease (NAFLD)

INTRODUCTION

1. Diabetes

Diabetes is a type of metabolic disorder characterized by hyperglycemia, which occurs due to insufficient insulin secretion or the inability of insulin to function properly. The high blood glucose levels can damage blood vessel walls, leading to macrovascular complications such as cardiovascular, cerebrovascular, or peripheral arterial disease, and microvascular complications such as retinopathy, neuropathy, or diabetic kidney disease. [1-3]

Diabetes is predominantly divided into two primary categories: Type 1 diabetes mellitus (T1DM) and Type 2 diabetes mellitus (T2DM). T1DM, previously referred to as juvenile diabetes or insulin-dependent diabetes, is a persistent disorder where the pancreas is incapable of producing insulin or produces it in very minimal amounts. [4, 5] T2DM, which is the most prevalent in adult, typically affects adults and arises when the body develops resistance to insulin or fails to produce an adequate amount of insulin. T2DM is characterized by increased insulin resistance, where cells are unable to effectively utilize glucose. [5, 6] It is not a single disease but encompasses a variety of disorders with different causes, all of which share hyperglycemia as a common factor. [3] Despite the diverse etiologies, they commonly exhibit insulin resistance. Therefore, insulin resistance serves as a quantitative indicator of insulin function, representing the most important precursor and a powerful predictor of the onset of T2DM.

T2DM is significantly influenced by environmental factors such as Westernized

dietary habits, which include high-calorie, high-fat, and high-protein diets, along with a lack of exercise and stress. Additionally, it can be caused by specific genetic defects, pancreatic surgery, infections, and medications. [5] According to statistics from the International Diabetes Federation (IDF), T2DM affects 280 million people worldwide, which accounts for 90% of all diabetes cases, and it is commonly known as a metabolic disorder often associated with obesity. The IDF reported that in 2020, approximately 537 million adults over the age of 20 had diabetes. The federation projects that this number will increase to 643 million by 2030 and reach 800 million by 2045. [7]

In South Korea, the prevalence of diabetes has been gradually increasing since the 1970s. According to the 2022 Diabetes Fact Sheet published by the Korean Diabetes Association, as of 2020, 1 in 6 adults aged 30 and above (16.7%) have diabetes. Among adults aged 65 and above, 3 in 10 (30.1%) are affected by the disease. [8] (Figure 1) The number of diabetes patients is expected to continue rising in the future.
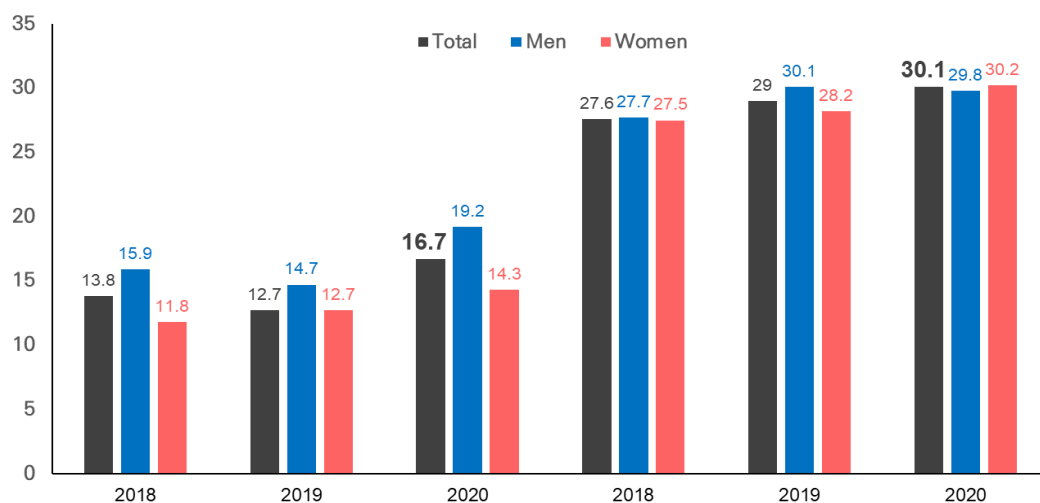
Figure 1 Prevalence of diabetes in South Korea (2020)

2. Pharmaceutical therapy

Pharmacological treatment for diabetes is broadly divided into oral anti-hypoglycemic agents and injectable anti-hyperglycemic agents. The choice of medication is made considering the patient's clinical characteristics, the efficacy and side effects of the drug, and costs. [9, 10]

In recent trends for oral anti-hyperglycemic agents, Sodium-glucose cotransporter-2 (SGLT-2) inhibitors have been introduced. notable examples include dapagliflozin, ipragliflozin, and empagliflozin. These medications work by inhibiting the reabsorption of glucose in the kidneys (SGLT-2 inhibitors prevent glucose from being reabsorbed in the renal tubules, allowing it to be excreted through urine). [11] This mechanism helps control blood glucose levels by increasing glucose excretion and is independent of insulin sensitivity and secretion. As a result, they are not significantly influenced by beta-cell dysfunction and insulin resistance. [12] Additionally, when used alongside other oral medications, they have a lower risk of causing hypoglycemia and, when combined with insulin, may reduce insulin-related weight gain while promoting weight loss by increasing glucose excretion. [11, 13, 14] These drugs not only help in controlling blood sugar levels but also assist in weight management and may even lower blood pressure. However, they can cause side effects such as thirst, polyuria, and dehydration due to osmotic diuresis induced by glucose excretion, and there is an increased risk of urinary tract infections due to higher glucose levels in urine. [13]

For injectable anti-hyperglycemic agents, Glucagon-like peptide-1 (GLP-1) receptor

agonists (GLP-1 RAs) have emerged as a new treatment for T2DM including Semaglutide, Liraglutide, and Dulaglutide, agents and insulin therapies. GLP-1 is an incretin hormone secreted by the L-cells in the intestine in response to the presence of nutrients or elevated blood glucose levels. It enhances insulin secretion in response to glucose without causing hypoglycemia. [15] However, most of GLP-1 RAs need to be administered either daily or weekly through subcutaneous injections, which can affect patient compliance. [16, 17] The net prices of GLP-1 RAs, after accounting for manufacturer discounts, range from $312 to $469 per month for type 2 diabetes. [18] These high costs are a significant concern for both patients and payers, especially given the large prevalence of obesity and type 2 diabetes. Additionally, GLP-1 agonist has been reported to increase the risk of diabetic retinopathy and gastrointestinal disturbances. [19-21]

In addition, dual and triple agonists have recently reported a new frontier in the treatment of T2DM, targeting multiple pathways. These multi-agonists such as Tirzepatide (dual agonist: GLP-1 and Gastric inhibitory polypeptide; GIP) or Retatrutide (triple agonist: GLP-1, GIP and glucagon receptor) aim to provide synergistic metabolic benefits, improving glycemic control and promoting weight loss more effectively than single-hormone therapies. [22] In clinical trial study, both Tirzepatide and Retatrutide have demonstrated significant efficacy in weight reduction and glycemic control, with tirzepatide also showing significant reductions in systolic blood pressure and improvements in lipid profiles. [23-25] As research continues, although these drugs represent a cornerstone in the management of T2DM, these

have several challenge and limitation such as efficacy variability, complexity of mechanisms, and regulatory hurdles.

Moreover, treatments for T2DM such as insulin, insulin secretagogues, thiazolidinediones, and sulfonylureas can lead to significant weight gain by altering glucose metabolism. [26, 27] Despite the remarkable advancements in oral anti-hyperglycemic agents, fewer than 30% of patients achieve adequate blood glucose control with medication alone. [8] This underscores the urgent need for non-pharmacological treatments for metabolic diseases, which are increasingly being recognized as a promising field for future development.

Given this context, there is a critical need for novel treatments that can maximize therapeutic effects while addressing the limitations of existing therapies for T2DM. This includes developing new mechanisms of action that can complement current drug therapies, providing more comprehensive management of these conditions.

3. *Non-pharmacological intervention*

Recent studies have shown that a high-fat diet, a major factor in the development of T2DM, causes the loss of tight junctions between epithelial cells in the duodenum, leading to increased intercellular gaps. [28] This results in changes to the gut microbiota and increased bacterial translocation, causing inflammation, and thickening of the duodenal lining. [29, 30] Other research indicates that a high-fat diet increases the whole intestine surface area and volume, as well as mucosa volume and crypt density. [30, 31] When the duodenal mucosa

5

thickens, there is an increase in the secretion of metabolic disease-related hormones such as GLP-1 and GIP from the K and L cells located in the duodenum. [32]

Based on these findings from previous studies, the duodenum has recently been highlighted as a key target for non-pharmacological treatment of metabolic diseases like type 2 diabetes and obesity. Investigations are being conducted into external interventions on the duodenum, such as surgical treatments like duodenal bypass surgery and non-invasive techniques like duodenal mucosal regeneration. [33] These approaches aim to modulate the duodenum's function and its role in metabolic regulation as promising alternatives to traditional drug therapies.

1) *Bariatric surgery*

Bariatric surgery is primarily performed for the treatment of obesity, but it also has a significant impact on T2DM, often leading to substantial improvement or remission of the disease. The relationship between bariatric surgery and T2DM is multifaceted, involving both weight-dependent and weight-independent mechanisms. The main types of bariatric surgery include Roux-en-Y Gastric Bypass (RYGB), Sleeve Gastrectomy, and Biliopancreatic Diversion with Duodenal Switch. [34] Among these, RYGB involves creating a small pouch from the stomach and directly connecting this pouch to the lower part of the small intestine, bypassing most of the stomach and the upper part of the small intestine. This procedure has been shown to result in marked and sustained weight loss, which is a primary driver for the

improvement in glycemic control and remission of T2DM. [35, 36] The American Diabetes

Association notes that bariatric surgery can lead to near or complete normalization of glycemia

in approximately 40-95% of patients with T2DM, depending on the type of surgery and patient

characteristics. [37]

There are several reasons why these duodenal function-related surgical procedures

are effective in metabolic improvement for patients with type 2 diabetes. The key mechanisms

include (1) increased incretin effect, (2) changes in gut microbiota, and (3) alterations in the

gut-brain axis. [34-36, 38] These mechanisms interact to contribute to diabetes improvement.

After RYGB surgery, the duodenum and part of the small intestine are bypassed, preventing

direct contact with food. As a result, the lower part of the small intestine secretes more incretin

hormones (such as GLP-1 and GIP). These hormonal changes are particularly pronounced in

procedures that bypass portions of the small intestine, such as RYGB, and contribute to the

rapid improvement in glycemic control by promoting insulin secretion and inhibiting glucagon

secretion [35, 36]

Additionally, duodenal exclusion alters the chemical environment of the gut by

preventing the release of bile acids and pancreatic enzymes into the duodenum. This change

in the chemical environment leads to a shift in the gut microbiota. Furthermore, the changes

in incretin hormones and gut microbiota affect gut-brain neural signaling, which helps regulate

appetite and satiety. [38]

Thus, bariatric surgery related to duodenal function contributes to diabetes

improvement through complex mechanisms involving physical and chemical changes in the gut environment. However, it is important to note that such surgeries come with risks such as bowel perforation and obstruction. Moreover, as irreversible surgical treatments, they require lifelong dietary restrictions and significant lifestyle adaptations.

2) *Recent application for Duodenal mucosal regeneration*

Duodenal Mucosal Regeneration (DMR) is a non-invasive endoscopic treatment technique primarily used to improve insulin resistance and enhance blood glucose control in patients with T2DM. [33, 39, 40] This procedure involves using a balloon catheter-type hydrothermal device (Revita, Fractyl Health, US) or a pulsed electric field device (ReCET, Endogenex, US) to ablate the abnormally thickened mucosal surface tissue in the duodenum and induce regeneration of the mucosa with healthy cells. (Figure 2)
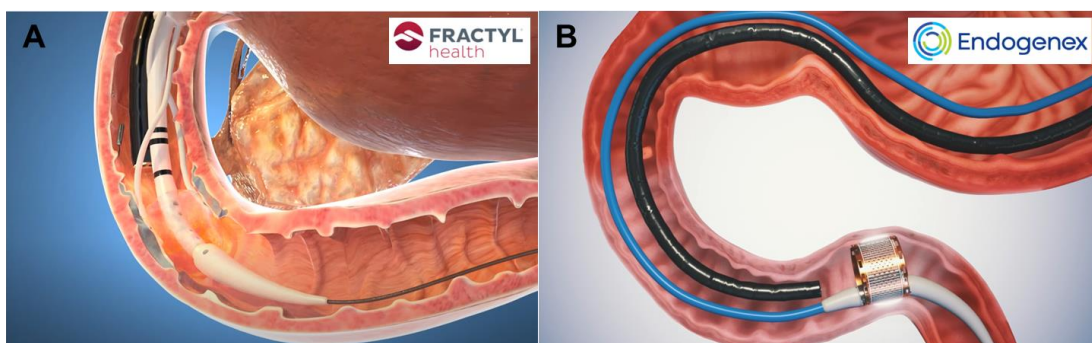
Figure 2 Schematics of existing devices used for duodenal mucosal regeneration: (A) Revita developed by Fractyle Health, (B) ReCET developed by Endogenex

In a study involving 36 patients with T2DM, DMR was performed using Revita from Fractyl Health. A single DMR procedure using Revita device resulted in improvements in

insulin resistance and a reduction in HbA1c by 0.9%, with these effects lasting for 12 months. [39] In another study using Endogenex's ReCET, DMR combined with GLP-1 RA therapy showed that 12 out of 13 patients were able to discontinue insulin therapy six months post-treatment, with their HbA1c levels reducing from 7.2% to 6.6%. [40] These findings suggest the potential for non-pharmacological treatment of type 2 diabetes.

However, the endoscopic treatments using Revita and ReCET require general anesthesia and fluoroscopy-guided operation of medical devices. The procedure typically takes about 60 minutes and is considered complex and technically demanding. [41] Additionally, potential complications such as irreversible damage to the duodenum due to high thermal exposure highlight the need for the development of more effective and safer duodenal non-pharmacological treatment platforms.

3) *Novel concept of duodenal mucosal regeneration therapy*

Photobiomodulation (PBM), previously known as light therapy, laser therapy, or Low-Level Laser Therapy (LLLT), refers to the use of specific wavelengths of visible light and near-infrared light to induce changes in human tissue by illuminating the tissues with light sources of appropriate wavelengths and intensities. [42, 43] Historically, it was used in medical devices intended for inflammation reduction, pain alleviation, advanced athletic performance, and improvement of general wellness. [42, 44] There is a growing body of research investigating the mechanisms of PBM and its therapeutic applications for various conditions

such as diabetes, brain injury, skin regeneration, pain relief, and targeting inflammation. Particularly, numerous studies have demonstrated the efficacy of external PBM using light in the 600 nm or 800 nm wavelength ranges to activate pancreatic functions and improve blood glucose levels, advanced insulin resistance, decreased fasting hyperinsulinemia, and regeneration of pancreas and liver showing promising results for the treatment of metabolic disorders such as type 2 diabetes. [45-54] Moreover, the use of external PBM has been linked to reductions in fat accumulation and inflammation within adipose tissue. [45, 49] These beneficial outcomes could be suggested to be due to increased adenosine triphosphate levels in mitochondria and an enhanced cellular response resulting from PBM therapy. [55, 56] However, in most PBM studies, light is externally irradiated to the animal model or cells, making it unclear whether the specific organ is targeted for treatment. As a result, experimental hypotheses of therapeutic mechanism based on these previous studies have not yet been clearly elucidated. In addition, in cases where targeted therapy is not feasible with external PBM, a relatively large amount of light exposure is required to reach deep-seated organs within the body (power density: 25–780 mW/cm2, energy diesity: 5–30J/cm2). Therefore, it is not suitable for practical application which designed for potential expansion considering the feasibility of large animal studies or clinical trials for human. [45-49, 52, 54]

In this study, we aim to validate the effects of DMR therapy targeting the duodenum through preclinical trials. We will meticulously analyze the resultant metabolic changes and alterations in gut microbiota to demonstrate the therapeutic efficacy of duodenal mucosal

regeneration. The research is structed into three primary phases evaluation of therapeutic effects using a catheter with Light Emitting Diode (LED)/Organic Light-Emitting Diode (OLED) light.

Evaluation of therapeutic effects using a catheter with LED point light:

We will apply a small catheter equipped with mini-LED chips emitting dual wavelengths at 630 nm and 850 nm to perform duodenal mucosal regeneration in type 2 diabetic rats. The therapeutic effects will be assessed to determine the efficacy of this approach.

Evaluation of therapeutic effects using a catheter with OLED surface light:

We will apply a small catheter equip with OLED surface light sources with a wavelength range of 600-700 nm for duodenal mucosal regeneration in type 2 diabetic rats. The therapeutic effects in this phase will also be evaluated to compared with the control group.

Safety and efficacy assessment in a type 2 diabetic large animal model:

A diabetic minipig model will be applied to assess the safety and efficacy of an endoscopically attached device incorporating mini-LED chips (630 nm/850 nm). This phase aims to ensure that the therapy is not only effective but also safe for potential larger scale applications.

By conducting these purposes of investigation, we will seek to establish a foundational understanding of DMR capacity to optimal duodenal mucosal regeneration and its broader impacts on metabolic health and gut microbiota.

MATERIALS AND METHODS

1. *Protocol of DMR experiment using mini-LED catheter (1):*

Diabetic Goto Kakizaki (GK) rats (11 to 12-week old, male) were purchased from Japan SLC Inc. (Hamamatsu, Japan). GK rats are spontaneously diabetic animal model of non-insulin-dependent diabetes mellitus characterized by progressive loss of β cells in the pancreatic islets with fibrosis. [57, 58] All animals were housed in individual cages under constant ambient temperature and humidity in a 12-hour light/dark cycle. This study was conducted in compliance with the guidelines for humane handling of laboratory animals and received approval from the Institutional Animal Care and Use Committee (IACUC no. 2020-12-247).

Triangular 5-cm effective 10 mini-LED chips were attached in each two dimensions in 2.5 mm diameter and 6 cm in length of polyurethane catheter. The LED light power source from the fabricated LED catheter was identified using a power meter (Newport 1936-R; Newport Corp., CA, United States). Catheter based radiofrequency ablation (RFA, 2.2cm length, 7W, 5 seconds Taewoong Medical) was applied for simulated duodenal mucosal regeneration because hydrothermal RFA probe was not commercially available in Korea. Due to the severe burning effect of RFA for duodenum and early death in prior energy settings in SD rats, duration of RFA was limited to 5 seconds. We performed a pilot study for choosing the optimal wavelength of LED for DMR.

Prior to performing DMR, all GK rats were administered inhalation anesthesia using

2% isoflurane (Hana Pharm, Hwaseong, Korea). After making an incision of the abdominal wall, the fabricated LED catheter was lubricated with lidocaine HCL jelly (Korea Pharma Co. Ltd, Seoul, Korea) and inserted into the duodenal bulb through a small incision in the duodenum, which was done once for several minutes of DMR during the entire observation period. DMR treatment using an LED catheter was performed once at the baseline during the entire observation period. During the procedure, the GK rat was placed on a heated operating table at approximately 40 degrees Celsius to prevent of hypothermia caused by exposure of internal organs. All internal organs except for the duodenum were covered with sterilized gauze and the gauze was frequently flushed with saline to prevent drying of the exposed organs. After the procedure, the incision in the duodenum was sutured with absorbable suture thread, and ketorolac (1 mg/kg) was administrated intramuscularly on the day of DMR therapy to prevent post-surgical pain. After the completion of the procedure, all GK rats thrived well without any complications except RFA group.

Experimental energy settings including 630nm, 850nm, dual (630nm/850nm), and RFA were evaluated in 1-week after duodenal intervention via gastrostomy using triangular shaped LED catheter with 2-illuminated dimension. The RFA probe and LED catheter were inserted into the duodenum through the incised stomach near to the pyloric sphincter. The 5cm length of the first part of duodenum was irradiated as follows the energy setting protocol. (Table 1) In 1-week follow-up study, oral glucose tolerance test (OGTT) was conducted at baseline and 1 week after in DMR with 2 dimensional illuminated LED in a triangular catheter

(irradiance, time; 630nm: 3.7 mW/cm^2, 600 sec; 850nm: 32.72 mW/cm^2, 100 sec; 630/850nm: 3.7/7.7 mW/cm^2, 500 sec), radiofrequency ablation (RFA) and sham control. For DMR with dual wavelength, 2 illuminated LED in duodenum was placed toward ipsilateral and medially located pancreas during DMR with dual wavelength. (Figure 3)

	Group	Wave-length [nm]	Time [s]	Voltage [V]	Current [mA]	Irradiance [mW/cm^2]	Energy density [J/cm^2]
1 week follow up	LED (630)	630	600	1.92	200	3.7	2.22
	LED (850)	850	110	1.45	300	32.72	3.60
	LED (630/850)	630	500	1.92	200	3.7	1.85
		850		1.45	75	7.7	3.85
	RFA		3	7 [W]	-	-	-
4 week follow up	LED (630)	630	600	1.92	200	3.7	2.22
	LED (630/850)	630	500	1.92	200	3.7	1.85
		850		1.45	75	7.7	3.85

Table 1. Parameters of duodenal mucosal regeneration using mini-LED catheter in GK rat

Based on the optimal results of duodenal LED DMR in 1-week follow-up study, the experimental energy settings including 630nm and multi-wavelength (630nm/850nm) were evaluated in 4-week after duodenal LED DMR. In the 4 weeks follow-up study, we performed the LED DMR using the catheter with four illuminated dimensions so as to irradiate the whole surface of duodenal mucosal. In 4-week follow-up study with duodenal mucosal regeneration with four dimensional illuminated LED as to irradiate uniformly whole surface of duodenal mucosa (Irradiance, time; 630 nm: 3.7 mW/cm^2, 600 s; 630/850nm: 3.7/7.7 mW/cm^2, 500 sec), OGTT was performed in baseline and 1 week and 4 weeks in duodenal mucosal regeneration 4 weeks follow-up study, control, and sham control group. (Figure 3)
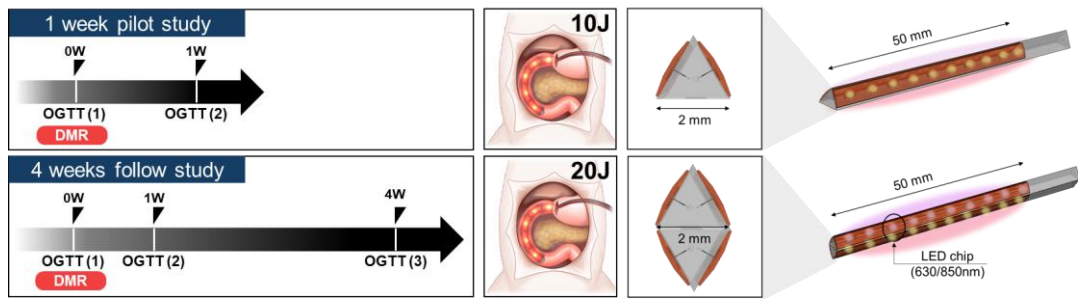
Figure 3 Experimental overview of the proposed LED catheter in 1- and 4-week follow up study

For the evaluation of thermal injury in the duodenal wall, an infrared camera (FLIR E6-XT; FLIR Systems Inc., OR, United States) was applied for thermal images in sham control, RFA, and each DMR group during procedure. (Figure 4)
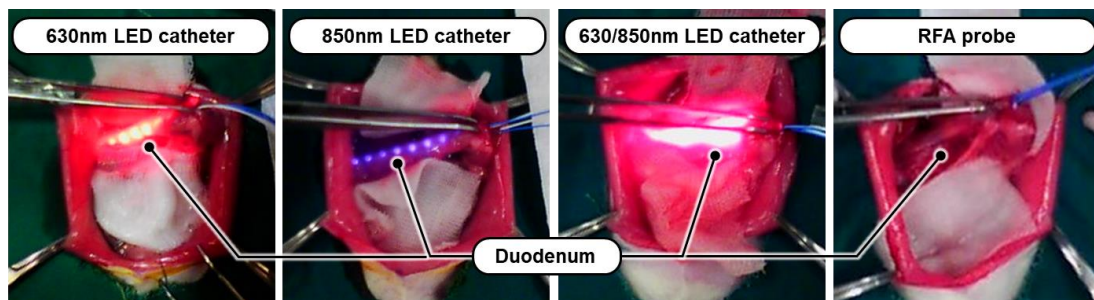
Figure 4 Photographs of duodenal mucosal regeneration using LED catheters and RFA probe in rat model

Gross of necropsy was performed for the evaluation of duodenal mucosal, liver, and pancreas in these groups after 4 weeks. The 850 nm wavelength illuminated catheter side was inserted toward the pancreas near the duodenum while performing the LED DMR.

2. *Protocol of Experiment using OLED catheter (2):*

Male diabetic GK rats (11- to 12-week-old) were purchased from Japan SLC Inc. (Hamamatsu, Japan). GK rats serve as a model for spontaneous non-insulin-dependent diabetes mellitus, characterized by a progressive decline in beta cells within the pancreatic islets, ultimately leading to fibrosis. [57, 58] To examine the physiological changes in disease models, which display a significant rise in hyperglycemia at 14-15 weeks and notable cellular deterioration at 16 weeks, we conducted a 4-week observation study using 11 or 12-week-old rats as the initial baseline. [58] All animals were housed individually under consistent ambient temperature and humidity conditions. The study was approved by the Institutional Animal Care and Use Committee (IACUC no. 2020-12-247) and followed the committee's guidelines for the humane treatment of laboratory animals.

In collaboration with the Korea Advanced Institute of Science and Technology, we developed an OLED catheter by rolling a flexible OLED into a cylindrical shape with a radius of 1.8 mm. The OLED is protected by upper and lower encapsulation layers, each measuring 6.06 µm in thickness, and secured to the cylindrical structure using adhesive tape with a thickness of 60 µm. To ensure biocompatibility and protection for both the internal OLED cell and the test subject, a 300 µm-thick biocompatible layer was applied to the external surface of the OLED catheter. The encapsulation layers on both the top and bottom consist of a symmetrical sandwiched structure, each made up of two dyads of parylene C (3 µm-thick) and Al2O3 (3 nm-thick), centered around the OLED. (Figure 5)
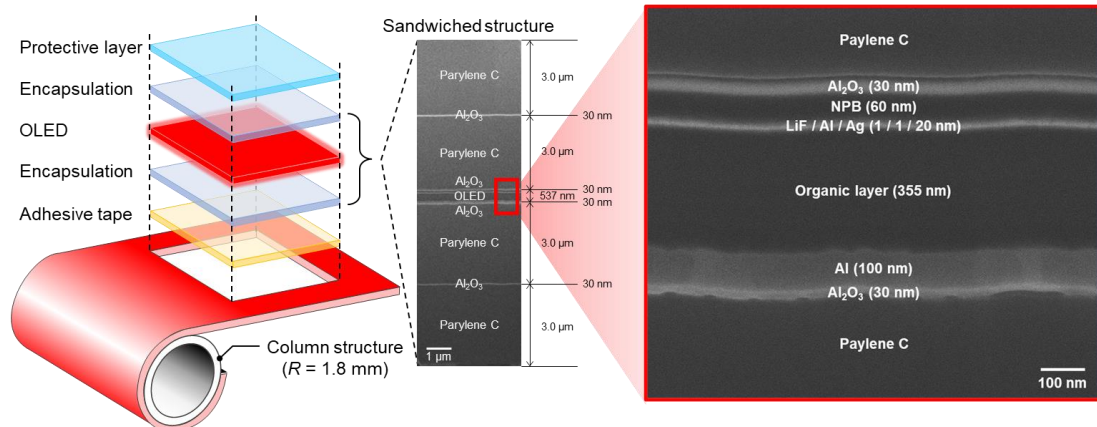
Figure 5 Overall configuration and FIB-SEM cross sectional image of the OLED catheter.

Fabricated OLED catheter was inserted into the duodenum through the incised superior portion of duodenum performing DMR for 10 minutes. The methodology is the same as the described above **experiment (1)** in detail. The OGTT was conducted at baseline, 1- and 4-week after DMR with OLED. (Figure 6) Necropsy was conducted after 4 weeks to assess the duodenal mucosa, liver, and pancreas. All rats in the case group treated with DMR (n=5) and the sham control group (n=4) survived the 4-week observation period without any significant complications, showing no signs of peritonitis or wound infection at the corresponding duodenal site.
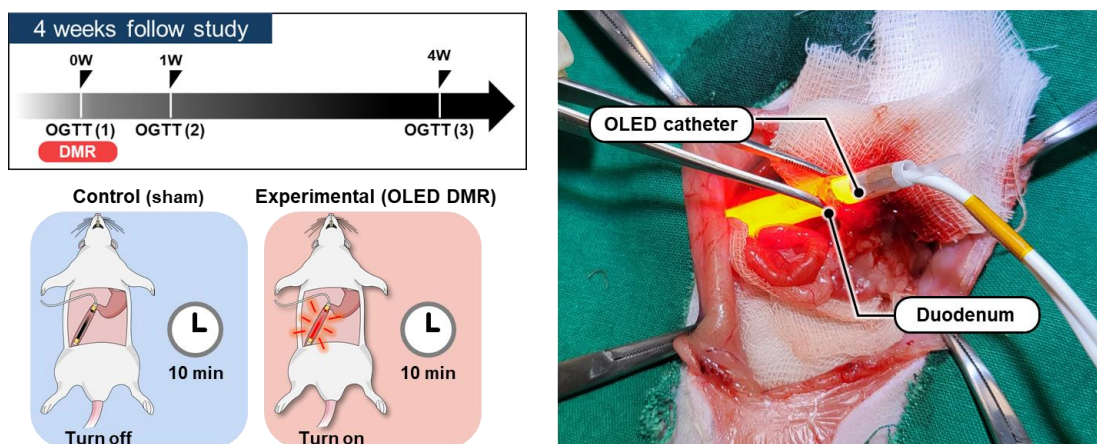
Figure 6 Experimental overview of the proposed OLED catheter in 4-week follow up study

3. *Protocol of Experiment using endoscopic DMR application (3):*

This study was approved by the Institutional Animal Care and Use Committee of our institution (2023-40-097) and conformed to University of Ulsan guidelines for humane handling of laboratory animals. Three mini pigs (Micropig, APURES Co., Ltd., Pyeongtaeksi, South Korea) weighing 32.0–34.5 kg (median, 34.5 kg, 10-12 months) were used in this experiment. All pigs were fed 600g of high fat high sucrose (HFHS) diet once a day. All pig were maintained at 22 ± 2 °C. The care and procedural protocols were conducted in accordance with the standards set by the National Institute of Health.

Due to the absence of a genetic large animal model for type 2 diabetes, this study chemically induced type 2 diabetes in three mini pigs through multiple low-dose/low-speed administrations of streptozotocin (STZ) combined with HFHS diet. Following the induction of hyperglycemia, HFHS diet was maintained for at least on month to induce insulin resistance and replicate duodenal mucosal thickening and inflammation. This diet consists of a feed mixture containing over 10% fat and 37% sugar. [59]

In this study, in collaboration with the Electronics and Telecommunications Research Institute, we developed a detachable distal application, featuring 473 mini-LEDs of 630 and 850 nm wavelength for DMR using upper endoscopy (EGD). The array of mini-LEDs equipped in DMR endoscopic application transferred onto flexible patch (3.0 cm by 6.4 cm, total area of 18.9 cm²) using Simultaneous Transfer and Bonding a simultaneous transfer process. [60] Additionally, the transferred LED patch module was encapsulated using an eco-

friendly silicone material (DOWSIL, EI-2888) for advanced aging performance and biocompatibility.

After 24 h of fasting and under the supervision of a veterinarian, the pigs were premedicated with 5 mg/kg zoletil and 1.5 mg/kg xylazine intramuscular. An endotracheal tube was placed, and anesthesia was administered by inhalation [2.5–3% isoflurane (Ifran®; Hana Pharm. Co., Seoul, Korea) with oxygen (2L per min) at 1:1]. All procedures were performed in the left lateral decubitus position. A linear gastro endoscopy (GIF-HQ290, Olympus Inc, Tokyo, Japan) was introduced into upper portion of duodenum. of pyloric and the upper duodenum. The DMR application attached to the tip of the endoscope illuminates the duodenum with light by toggling the power on and off at 90-second intervals for a total duration of 720 seconds. During this process, the light power output (2.6 Vrms, 400 Hz) at a wavelength of 630nm is 17.82 mW/cm², and the light power output (2.0 Vrms, 400 Hz) at a wavelength of 850nm is 97.04 mW/cm². After performing DMR for 12 minutes, the treatment area is observed, and the procedure is concluded. One week after the DMR procedure, the recovery status of the duodenal mucosal damage at the treatment site is examined via endoscopy. (Fasting and anesthesia are conducted as described previously) OGTT in the large animals are conducted baseline and at 1 week, 3 weeks, and 6 weeks after DMR. (Figure 7)
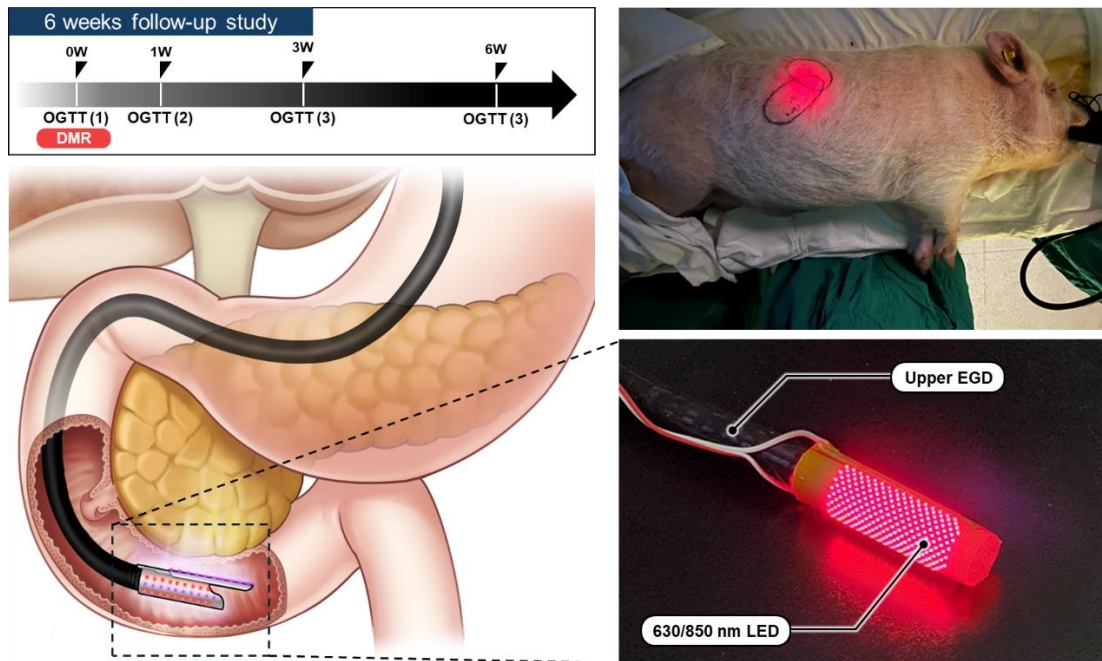
Figure 7 Experimental overview of the proposed endoscopic cap with mini LED in 6-week follow up study in diabetic mini pig

4. Oral Glucose Tolerance Test (OGTT) Procedures in Animal Studies

After fasting overnight (16-18 hours), an OGTT was conducted twice in pilot study in GK rats (0-, 1-week after DMR), 4-week follow up study using LED/OLED catheter in GK rats (0-, 1-, 4-week after DMR) and 6-week follow up study in diabetic mini-pig study (0-, 1-, 3-, 6-week after DMR). Blood for baseline (0 min) was collected from the tail vein in GK rats. Following baseline, the solution of 25% dextrose (0.01 mL/g) was orally administered at 2.5g/kg. The blood collection was conducted at 30, 60, 120 minutes in EDTA coated collecting tubes while blood glucose level was measured at 15, 30, 60, 90, and 120, with or without 180 minutes using instant blood glucose meter (ACCU-CHEK, Roche, Mannheim, Germany).

5. *Biochemical and Hormonal Analysis Procedures*

All biochemical and hormonal parameters were assessed in plasma samples obtained during the OGTT. The chemical analysis involved measuring the activity concentrations of liver enzymes such as cholesterol, alkaline phosphatase (ALP), alanine aminotransferase (ALT), and aspartate aminotransferase (AST) using the 7189 Clinical Analyzer (HITACHI, Tokyo, Japan). The hormonal parameters including insulin, GLP-1 and GIP were estimated using following enzyme-linked immunoassay (ELISA) kits, respectively. Multi Species GLP-1 Total ELISA (EZGLP1T-36K, Merck Millipore, Burlington, Massachusetts, US), Rat/Mouse GIP (total) ELISA (EZRMGIP-55K, Merck Millipore, Burlington, Massachusetts, US), Rat Insulin ELISA Kit (CC-90010, Crystal chem, Elk Grove Village, Illinois, US). GLP-1, GIP and insulin concentration were calculated following the manufacturer's instruction. Each assay was conducted in duplicate using the specified samples.

6. *Histological Examination and Staining Protocols*

Histologic examination of duodenum (PC: positive treated tissue, NC: negative treated tissue), liver and pancreas were performed after necropsy. The excised tissues were fixed in 10% neutral buffered formalin, then rinsed with tap water for about 2 hours to remove the formalin. The tissues were then dehydrated in the graded ethanol and cleared in xylene using a tissue processor (Shandon Diagnostics Ltd., Excelsior AS) and embedded into paraffin

blocks using a paraffin embedding station (Leica, EG1150H). Following this, the tissues were

embedded in paraffin, and 3 μm thick sections were cut using a rotary microtome (Leica,

RM2255). Sections were prepared onto the glasses. The hematoxylin and eosin (H&E) staining,

Masson trichrome (MT) staining and Multiplex Immunohistochemistry (IHC) staining were

performed. Multiplex IHC staining, scanning, and analysis were conducted by prismCDX Co.,

Ltd (Gyeonggi-do, Korea). Formalin-fixed, paraffin-embedded blocks were sectioned into 3-

μm slices. The slides were heated in a dry oven at 60°C for at least one hour, followed by

multiplex immunofluorescence staining using a Leica Bond Rx™ Automated Stainer (Leica

Biosystems). The table summarizes the antibodies and fluorophores used. Briefly, the slides

were dewaxed with Leica Bond Dewax solution (#AR9222, Leica Biosystems) and underwent

antigen retrieval with Bond Epitope Retrieval 2 (#AR9640, Leica Biosystems) for 30 minutes.

The list of the antibody and fluorophore used is summarized in the table. Briefly, the slides

were dewaxed with Leica Bond Dewax solution (#AR9222, Leica Biosystems), followed by

antigen retrieval with Bond Epitope Retrieval 2 (#AR9640, Leica Biosystems) for 30 minutes.

The staining proceeds in sequential rounds of blocking with antibody diluent / block

(ARD1001EA, Akoya Biosciences), followed by primary antibody incubation for 30 minutes

and Goat Anti-Rabbit IgG H&L (HRP polymer) (ab214880, Abcam) incubation for 10 minutes.

Antigen visualization was achieved using tyramide signal amplification (Akoya Biosciences)

for 10 minutes. Following this, the slides were treated with Bond Epitope Retrieval 1

(#AR9961, Leica Biosystems) for 20 minutes to remove bound antibodies before proceeding

to the next step in the sequence. The process from the blocking step to the antigen retrieval step is repeated for every antibody staining. Nuclei were stained with DAPI (62248, Thermo Scientific) for counterstaining after the last round of antigen retrieval. The slides were coverslipped using ProLong Gold antifade reagent (P36935, Invitrogen). H&E stained, and MT staining sections were digitized using a slide scanner (VS200; Olympus, Tokyo, Japan). The MT staining section in liver tissue was examined to measure interstitial collagen volume fraction (blue dyed) and corresponding area occupied (red dyed) using image analysis software (VS20S-DESK v3.2; Olympus, Tokyo, Japan). The insulin IHC stained pancreatic section was observed using the software (VS20S-DESK v3.2; Olympus, Tokyo, Japan) to estimate number and size of stained islet cells. Multiplex stained slides were scanned using the Vectra Polaris Automated Quantitative Pathology Imaging System (Akoya Biosciences) at 20x magnification. Representative images for training were selected in Phenochart (Akoya Biosciences), and an algorithm was created in the inForm Image Analysis software (Akoya Biosciences). Multispectral images were unmixed using the spectral library in inFome software. Based on DAPI staining, each single cell was segmented and phenotyping was performed according to the expression compartment and intensity of each marker. After designating the region (ROI, region of interest) to be analyzed on the tissue slide, the same algorithm created in this way was applied and batch-running. The exported data is consolidated and analyzed in R software using the phenoptr (Akoya Biosciences) and phenoptrReport (Akoya Biosciences) packages.

To measure spatial cell to cell distance, nearest neighbor analysis was used to calculate the distance between two cells located closest to each other, and count within analysis was used to calculate the percentage of other cell types within a few 15, 30μm radius of one specific cell.

7. *Microbiome analysis*

Total genomic DNA was extracted from fecal samples using the FastPrep-24 instrument (Qbiogene, MP Biomedicals, Illkirch, France) following the manufacturer's protocols. The V4 segment of the 16S rRNA gene was amplified for dual indexing and pooled using 515F and 806R primers. The analysis was performed on the Illumina iSeq100 platform. Raw reads were initially examined for quality, and those with a quality score below Q25 were filtered out using Trimmomatic version 0.32. Non-specific amplicons for 16S rRNA encoding were detected using nhmmer in the HMMER software (version 3.2.1) with HMM profiles. Unique reads were isolated, and redundant reads were merged with these unique reads using the derep_fulllength command in VSEARCH. Chimeric reads were filtered based on reference comparisons using the UCHIME algorithm and the non-chimeric 16S rRNA database from EzBioCloud. De-novo clustering to generate additional Operational Taxonomic Units (OTUs) was performed using the cluster_fast command. Further analyses, including diversity assessments and biomarker discovery, were conducted by CJ Bioscience, Inc. (Seoul, South Korea).

8. *Statistical analysis*

Continuous variables were expressed as means with interquartile range (IQR). An unpaired t-test and ordinary one-way ANOVA test were used to examine the difference between DMR group and others. In each same group, Wilcoxon test and Kruskal-Wallis test were conducted to evaluate the differences by 1- or 4-week follow up. For all analyses, statistical significance was determined using a two-sided P-value of < 0.05. Statistical analyses were conducted using GraphPad Prism 9.0.0 software (GraphPad Software Inc., San Diego, CA, United States).

RESULTS

1. Results from Experiment (1):

We quantified the optical characteristics in the catheter-type DMR application with LED chips. Voltage-current-luminance was measured for the 630 (Figure 8A) and for the 850 nm (Figure 8B). Radiant power applied voltage were quantified using a power meter (Newport 1936-R, Newport Corp., United States) at 630 nm (Figure 8C) and 850 nm (Figure 8D). Under the applied energy conditions in this experiment, it was confirmed that the temperature was maintained at a maximum of 55 degrees for the 630 nm single catheter, 48 degrees for the 850 nm single catheter, and 55 degrees for the 630/850 nm dual-wavelength catheter. (Figure 8E)
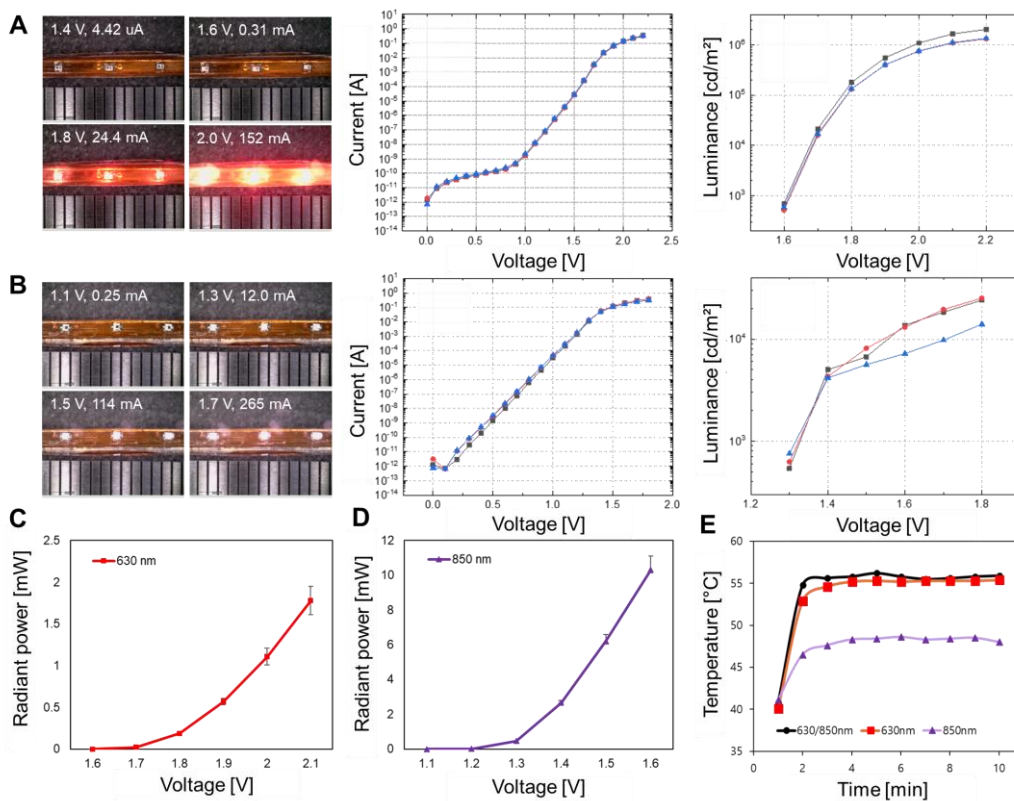
Figure 8 The optical and thermal properties of LED catheter: current [A] – Voltage [V] – Luminance [cd/m^2] at **(A)** 630 nm and **(B)** 850 nm wavelength, radiant power for **(C)** 630 nm and **(D)** 850 nm wavelength and **(E)** temperature characteristics of the mini-LED catheter**.**

Median procedure time including surgical incision, catheter intubation in duodenum, and closure for DMR or sham control was surgical incision 32.4 minutes (IQR: 29.1-35.0) in 1-week pilot study, and 29.6 minutes (IQR: 25.0-33.3) in 4-week follow-up study, respectively. All rats including case group applied DMR with LED and sham control well survived during and after the procedure without any complications and signs of sepsis, peritonitis, or wound infection. In the RFA group in a pilot study, four types of energy setting were performed as different irradiated time for 30, 20, 10 and 5 seconds respectively (30 sec; n=2, 20 sec; n=3, 10 sec; n=4, 5 sec; n=5). Among the energy settings depending on time variable, only five rats that were performed for five seconds could survive with mild intestinal stenosis in necropsy after 1-week following duodenal RFA. The other rats (n=9) applied with RF probe (7W, 5 sec) died the day after the implementation due to several intestinal obstructions. No significant change of body temperature was seen in the LED-DMR group compared to the RFA group.

Figure 9 shows the results of the pilot study related to OGTT test, body weight change, biochemistry, and histological analysis. DMR with multi-wavelength (630/850 nm) treated rats showed better glucose tolerance compared to all other study groups, as shown by -9.7% of lower area under curve (AUC) in glucose level in an OGTT curve ($P < 0.01$) and lower 15- and 30-minute time point than sham control ($P < 0.005$ for both). There were no significant differences of AUC in glucose on the OGTT curve in sham control, RFA, 630 nm and 850 nm groups after 1-week, even though duodenal LED DMR with 630 nm group and RFA showed lower glucose level at 15- ($P < 0.005$), 30-minutes ($P < 0.05$) and 120-minutes

(*P* < 0.005) relatively. (Figure 9)
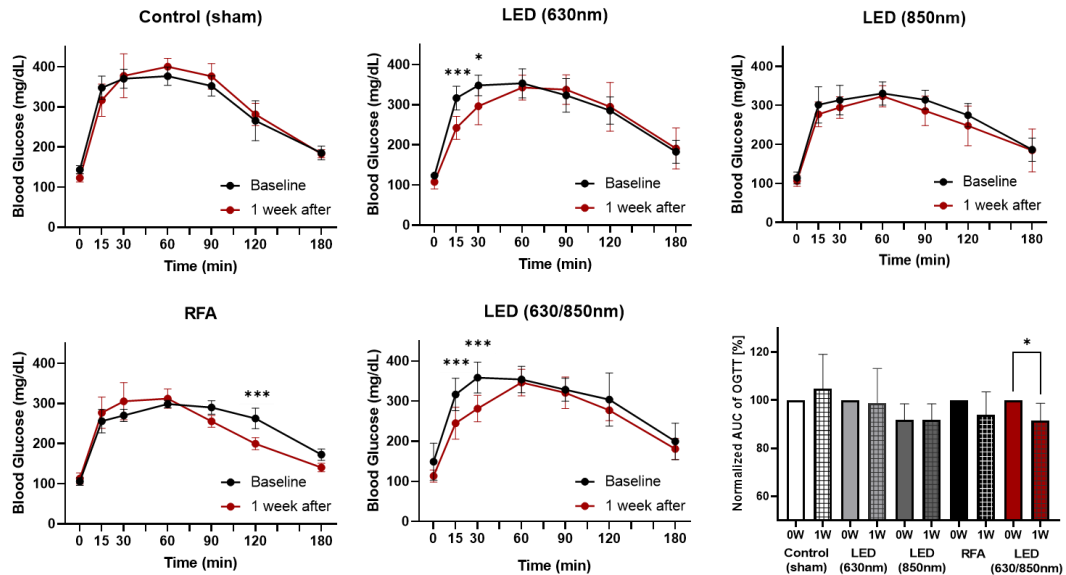
Figure 9 Glycemic curve during oral glucose tolerance test (OGTT) and normalized area under curve in comparison of baseline and 1 week after with sham control, DMR with 630 nm, DMR with 850 nm, radiofrequency ablation and DMR with LED (630/850nm).

	Area under curve (AUC)			
	Baseline	1 week	Diff of AUC (SD) [%]	
Contorl (sham)	53,445	56,623	4.84 (14.2)	N.S
LED (630nm)	51,573	50,531	−1.2 (14.4)	N.S
LED (850nm)	49,204	46,525	−5.33 (9.5)	N.S
RFA	44,966	42,113	−6.04 (9.5)	N.S
LED (630/850nm)	53,577	48,789	−9.67 (7.85)	*

Table 2 In comparison of normalized glucose AUC during OGTT between baseline and 1 week after with sham control, DMR with 630 nm, 850 nm, 630/850 nm and RFA group.

In comparison to sham control, only the dual wavelength LED DMR group was significantly lower in body weight gain without the change of food intake (Figure 10A, *P* < 0.05). In histologic analysis, the collagen deposition presenting blue areain the liver tissue

from dual wavelength LED DMR group was investigated at a lower value (0.01%) than that

from the sham control (0.16 %) and RFA group (0.24 %) without statistical significance

(Figure 10B). Sham-control and DMR groups showed no significant difference of AST and

ALT level compared baseline to 1 week after DMR. The level of cholesterol and ALP of at 1

week after were significantly less than the level at baseline in dual wavelength LED DMR

group and sham control (cholesterol: $P < 0.05$, ALP: $P < 0.01$) (Figure 10C).
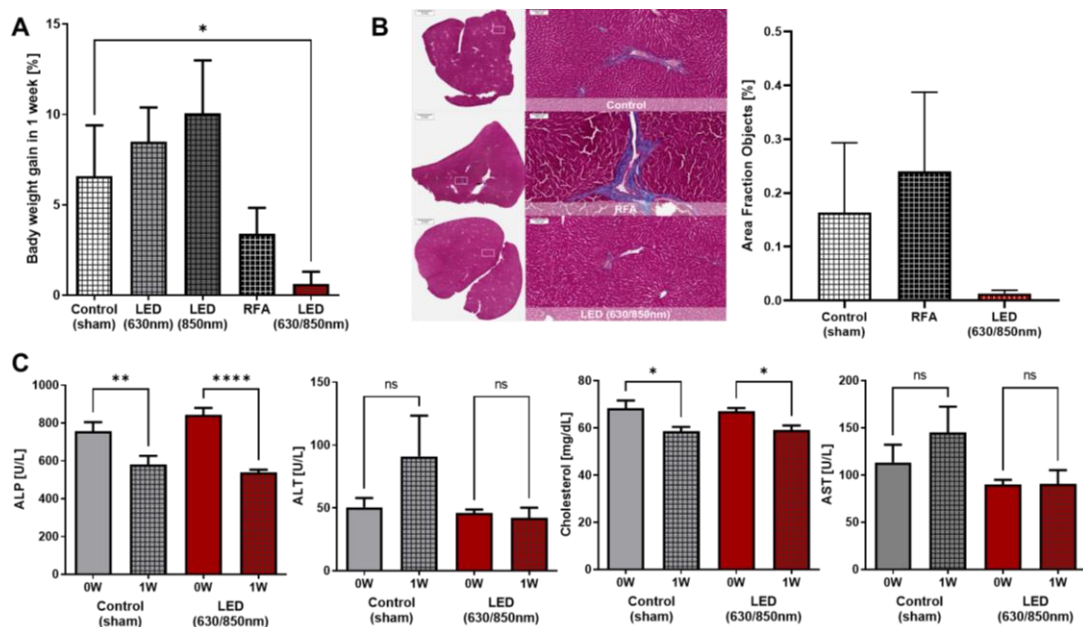
Figure 10 Effects on metabolic parameters in pilot study: (A) The percentage of body weight gain after the end of the experiment in 1 week follow-up. In accordance with histological images of MT staining of the liver tissue, collagen deposition in the liver tissue **(B)** with dual wavelength LED DMR was the lowest compared with sham control and RFA. **(C)** In comparison with the biochemistry parameters of AST, ALT, ALP and cholesterol level from sham control and DMR with dual wavelength between 0- and 1-week after.

Based on the results of 1-week pilot study, 630 nm, 630/850 nm was selected for

DMR with LED in 4-week follow-up study. After 1 week of treatment, there were no

significant differences in glucose levels in the OGTT curve compared to 0 week in control, sham control, and 630 nm groups. However, the dual wavelength LED DMR group showed a significantly lower glucose level at 15- ($P < 0.05$), and 30-min ($P < 0.05$) time points after 1 week and the treatment effects were maintained at 15- ($P < 0.05$), 30- ($P < 0.005$) and 60-min ($P < 0.01$) time points for 4 weeks (Figure 11). In accordance with this, glucose AUC of dual wavelength LED DMR group at both periods were significantly lower than baseline as shown by 11.68% (P < 0.01) lower in 1-week after and 14.50% (P < 0.005) lower in 4-weeks after relatively (Figure 11, Table 3).
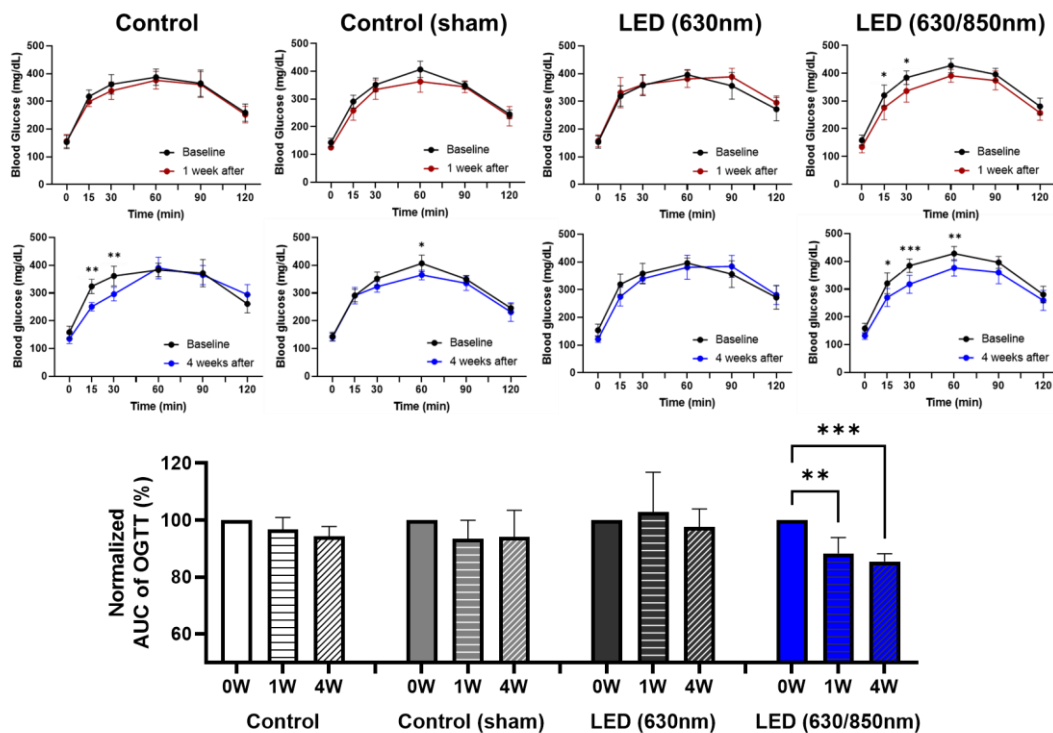
Figure 11 Glycemic curve during oral glucose tolerance test (OGTT) and normalized area under curve in comparison of baseline, 1 week and 4 weeks after with sham control, DMR with 630 nm and DMR with LED (630/850nm).

	Area under curve (AUC)						
	Baseline	1 week	4-week	Diff of AUC [%]			
				1-week (SD)		4-week (SD)	
Control	40,508	39,159	38,130	−3.28 (4.00)		−5.72 (3.62)	
Control (sham)	39,741	37,134	37,161	−6.55 (6.36)		−6.21 (9.32)	
LED (630nm)	40,872	41,789	39,827	2.90 (13.84)		−2.49 (6.49)	
LED (630/850nm)	44,013	38,882	37,639	−11.68 (5.42)	**	−14.50 (2.46)	***

Table 3 Normalized AUC of glucose OGTT in comparison of 0- versus 1-week, and 0- versus 4-weeks after with control, sham control, DMR with 630 nm and DMR with dual wavelength-LED (630/850nm).

Even though, there was no difference in the percentage of body weight gain among all treatment groups (Figure 12A). dual wavelength LED DMR group showed significantly reduced the levels of liver enzymes such as AST ($P < 0.05$) and ALT ($P < 0.01$) at 4 weeks post-treatment compared to baseline, which were not shown in control and sham control (Figure 12B).
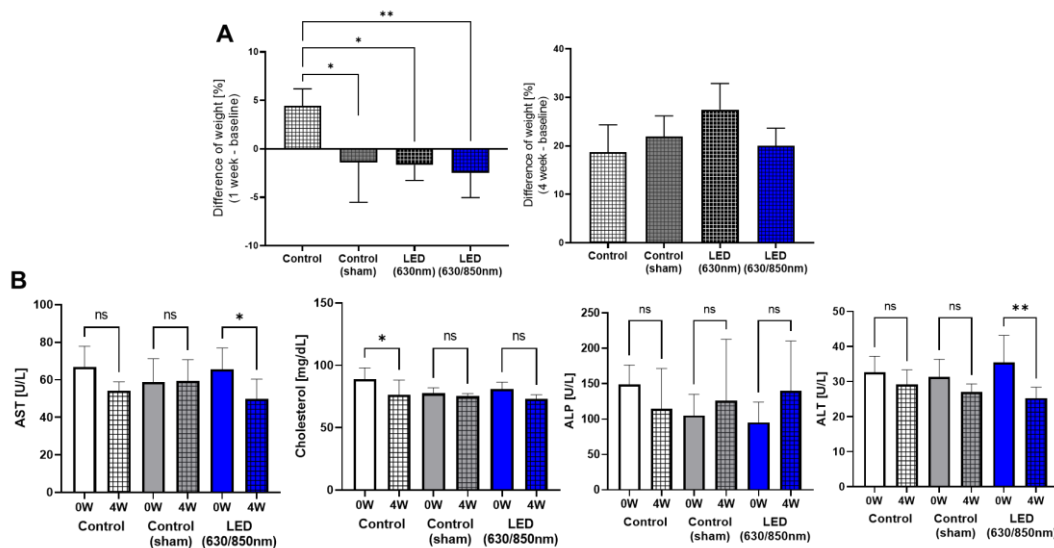
Figure 12 (A) The percentage of body weight gain after the end of the experiment in 1 week follow-up. **(B)** In comparison with the biochemistry parameters of AST, ALT, ALP and cholesterol level from sham control and dual wavelength LED DMR between 0- and 1-week after.

The progressive loss of beta cells in the pancreatic islets with fibrosis was clearly observed in the control group. However, the pancreatic islets were relatively well preserved and expression of insulin in IHC was increased at 4 weeks after treatments in the dual wavelength LED DMR group (Figure 13A). The percentage of β-cell areas within each pancreatic section were significantly greater in the dual wavelength LED DMR group ($P < 0.01$) compared to the control group (Figure 13B). There was no significant difference of collagen deposition in the liver among all treatment groups. No statistically difference in the expression of GIP and GLP-1 in duodenal villi among control, sham control, and dual wavelength LED DMR on IHC staining (Figure 13C). No definite mucosal abnormality or duodenal wall injury was seen in the dual wavelength LED DMR group.
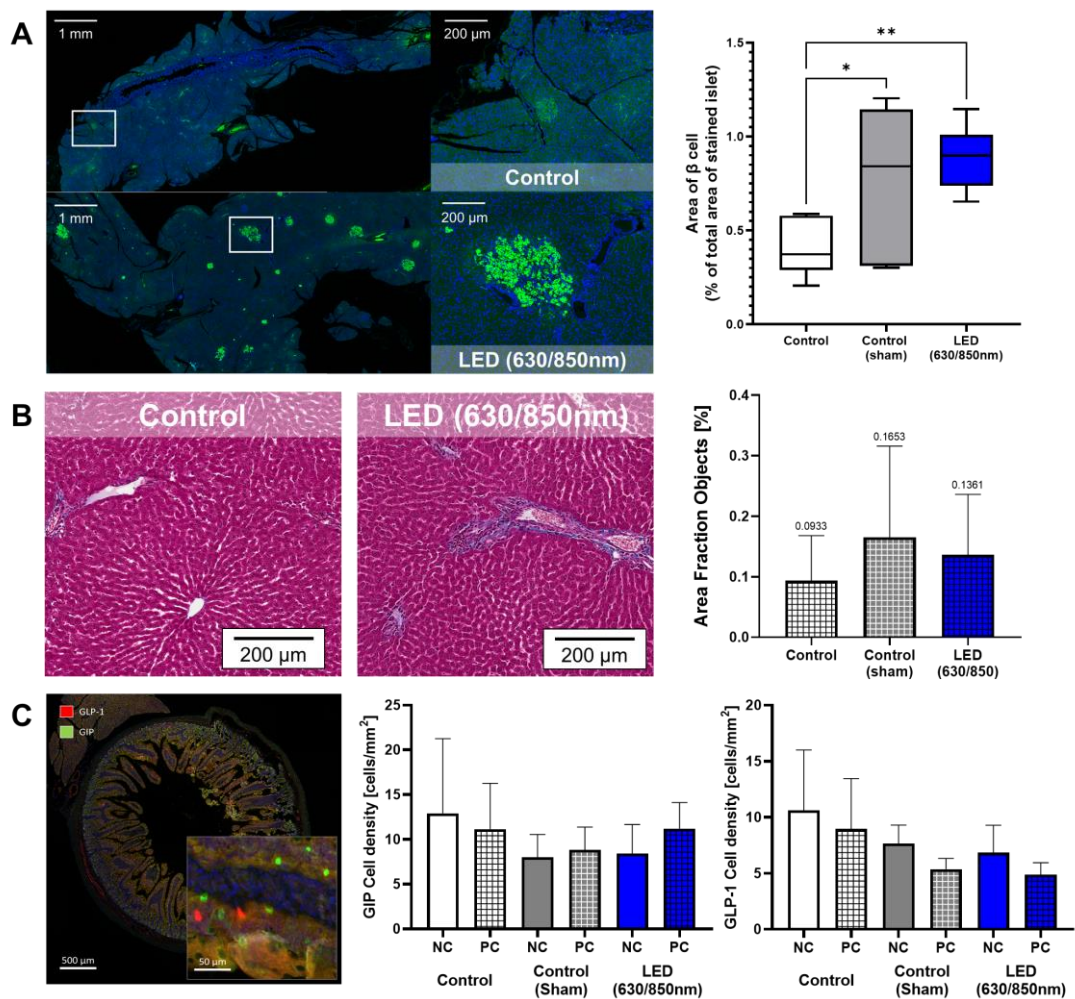
Figure 13 Comparison of staining results in control and experimental groups: (A) quantification of β-cell activity using insulin-targeted immunohistochemistry in pancreatic tissue, **(B)** quantification of fibrosis through collagen area using MT staining in liver tissue, and **(C)** quantification of mucosal cell activity using GIP and GLP-1-targeted multiplex immunohistochemistry in duodenal tissue.

As a result of the alpha-diversity analysis of the control group, bacterial species diversity increased after 1 week. However, after 4 weeks, the trend returned to baseline levels. Similarly, in the sham control group, species diversity increased after 1 week compared to baseline, and after 4 weeks, the diversity pattern remained similar to that observed after 1 week.

In contrast, the dual wavelength LED DMR group showed different alpha-diversity analysis results. In this group, species diversity decreased after 1 week compared to before the DMR with LED, and although there was a slight increase after 4 weeks, the diversity was still lower than before the DMR with LED (Figure 14A).

The beta-diversity analysis using the Unifrac distance metric in the three groups (control, sham control, dual wavelength LED DMR group) showed that the gut microbiota at different time points was not clearly distinguishable (Figure 14B). Next, the percentage of bacterial taxa differentiating the gut microbiota was calculated according to the period after DMR with LED in the three groups. The gut microbiota of the control group was predominantly composed of Firmicutes, Bacteroidetes, Proteobacteria, and Actinobacteria at the phylum level. After 1 week in the control group, Firmicutes and Proteobacteria decreased, while Bacteroidetes increased. The phylum-level composition in the sham control group was similar to that of the control group. After 1 week of dual wavelength LED DMR, Firmicutes decreased, and Bacteroidetes and Proteobacteria increased. However, no significant change in gut microbiota composition at the phylum level was observed over time in the dual wavelength LED DMR group (Figure 14C).

At the family level, the most abundant microbiome in the three groups was Erysipelotrichaceae, belonging to Firmicutes, followed by Muribaculaceae, belonging to Bacteroidetes (Figure 14D). Through LEfSe analysis, significant changes in gut microbiota at the genus level before and 1 week after dual wavelength LED DMR were presented as a

taxonomic bar chart (Figure 15E-F). Five genera (Bacteroides, Escherichia, Parabacteroides, Allobaculum, Faecalibaculum) were significantly enriched after 1 week in the dual wavelength LED DMR group ($P < 0.05$). Notably, Bacteroides acidifaciens significantly increased after 1 week in this group. On the other hand, five genera belonging to Lachnospiraceae significantly decreased after 1 week (Figure 16G, $P < 0.05$).

In the control group, three genera (KE1591_g, PAC001516_g, PAC001165_g) were significantly enriched after 1 week ($P < 0.05$). In the sham control group, six genera (Bacteroides, Pseudoflavonifractor, Eubacterium_g23, Parabacteroides, Escherichia, Alistipes) were significantly enriched after 1 week ($P < 0.05$).
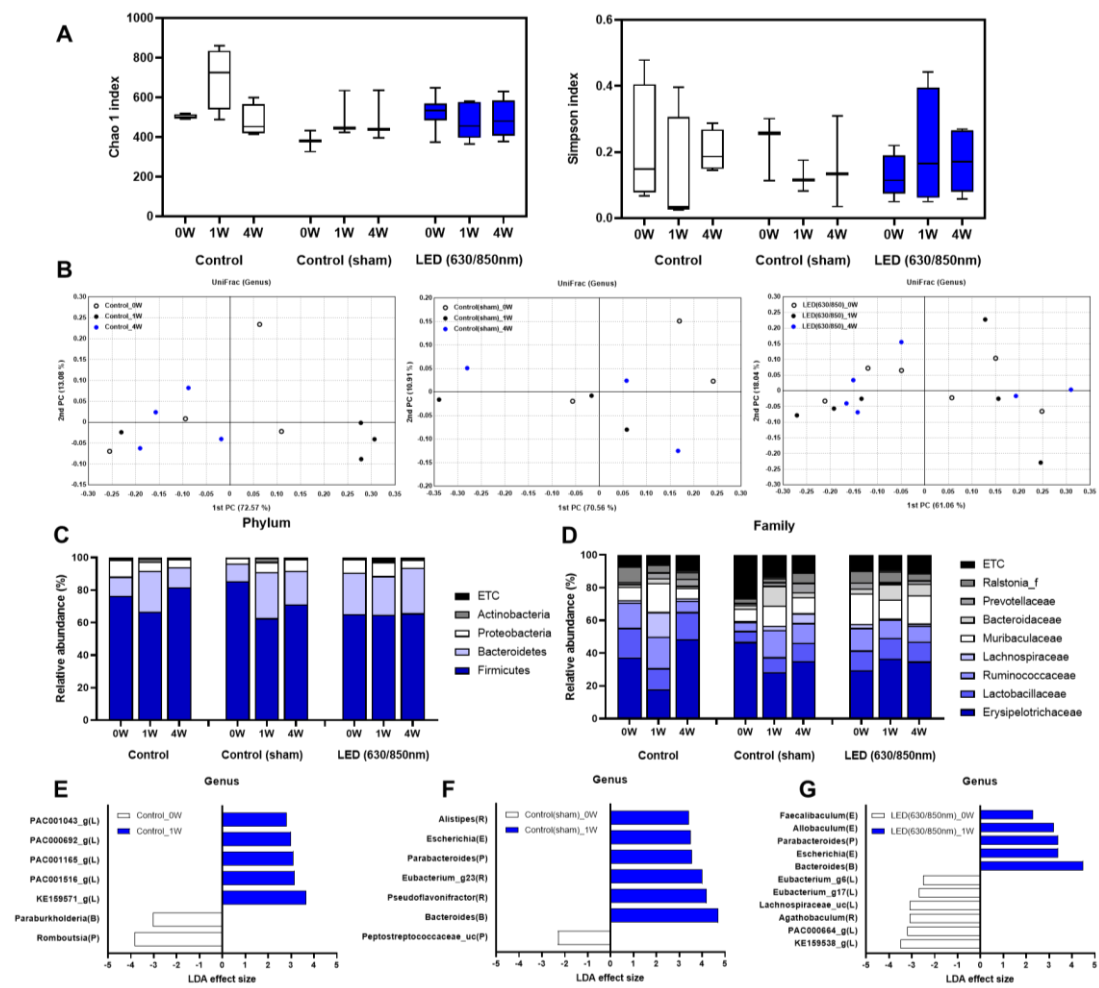
Figure 14 Comparison of gut microbiome after irradiation DMR with-LED in GK rats. (A) Chao1 index and Simpson index reflecting the richness and diversity of gut microbiome. (B) Principal coordinate analysis (PCoA) plot using Unifrac distance of gut microbial communities obtained from three groups at the different time points. (C) Composition profiles of the gut microbiome at phylum level in control GK rat, sham and dual LED. (D) Main fecal microbiomes of family level in three groups at the different time points. (E-F) Differentially represented genus between 0W and 1W in each group by linear discriminant analysis effect size (LEfSe) analysis.

To evaluate the underlying mechanisms of the altered gut microbiome from 1 to 4 weeks in the DMR with dual wavelength group, the differences in serum GIP, GLP-1, insulin, and insulin resistance (HOMA-IR) were identified between the 1-week and 4-week periods.

Although the differences in serum GIP, GLP-1, and insulin levels during the OGTT were not significant between baseline and post-treatment periods, the AUCs for GLP-1 (P < 0.01) and insulin (P < 0.01) between 1-week and 4-week treatments were significantly higher in the sham control and dual wavelength LED DMR groups compared with the control group. Additionally, insulin resistance significantly decreased at both 1 week (P < 0.005) and 4 weeks (P < 0.01) after dual wavelength LED DMR treatment compared with baseline. The AUCs of serum GIP levels during OGTT did not differ before and after each treatment (Figure 15).
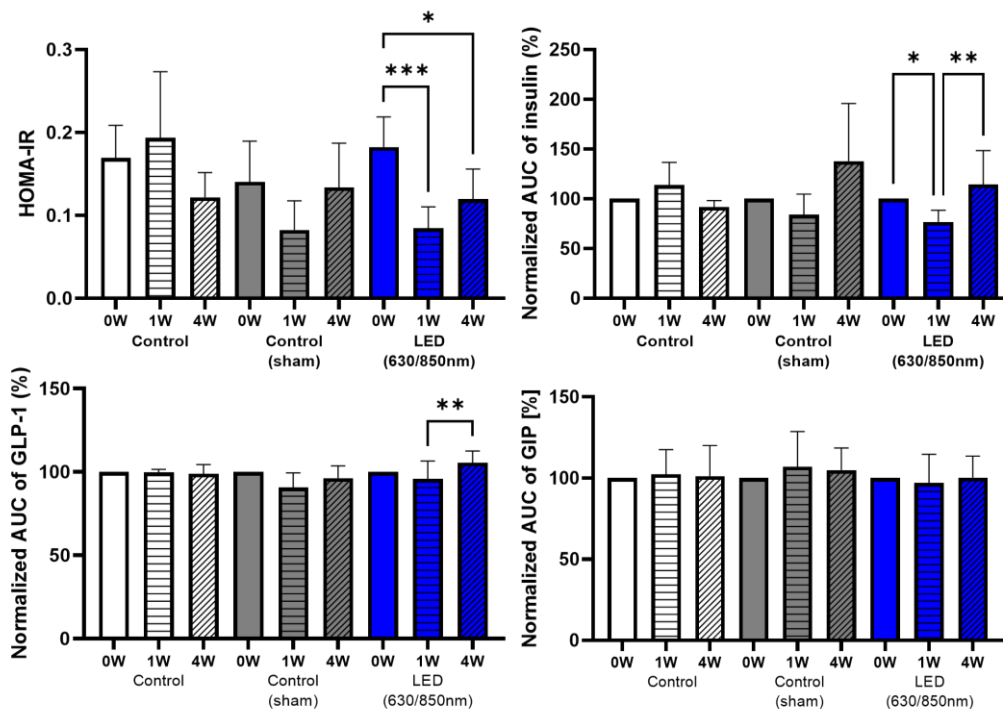
Figure 15 Comparison of **(A)** HOMA-IR in control, sham control and DMR with LED (630/850nm) group showing baseline, 1- and 4-week after DMR. Normalized the area under the curve for **(B)** insulin, **(C)** GLP-1 and **(D)** GIP hormone level during OGTT in control, sham control and DMR with LED group between baseline, 1- and 4-week after DMR. The data are presented as the mean ± SEM. ANOVA with the Bonferroni's post hoc test was used for statistical analysis. * p < 0.05, ** p < 0.01, *** p < 0.005

2. Result from Experiment (2):

We drove the OLED catheter with a constant current of 28 mA, and the voltage under the condition was about 5 V (Figure 16A). At this time, the radiance of the OLED catheter was 0.58 W/m^2/sr, which corresponded to a radiant power of 1.33 mW considering the area of the light source and the light distribution (Figure 16B). Since we turn on the light from the OLED catheter which were inserted into the duodenum of GK rats for 10 minutes, energy of about 798 mJ was finally delivered. To assess the encapsulation characteristics of the OLED catheter, we performed a lifetime test by immersing the device in a PBS solution. (Figure 16C). The OLED catheters were emitted light both in PBS solution maintain at 38°C and in the air for control. Since the relative radiance of the two OLED catheters commonly decreased by less than about 5% for about an hour, this seems to be due to the inherent characteristics of OLED materials, not the water permeation factor. Additionally, we monitored the operating temperature of the OLED catheter for 10 minutes, corresponding to the duration of the actual animal experiment. (Figure 16D). The temperature change of the OLED catheter was made from room temperature to 35.8 °C, and the inset of the Fig. 4E corresponds to the thermal imaging camera image at the highest temperature. Since the body temperature of a normal rat is about 35.7 to 38 °C [61] and the operating temperature range of the OLED catheter does not exceed this range, we do not investigate any additional side effects such as low-temperature burns caused by the device during animal experiments.
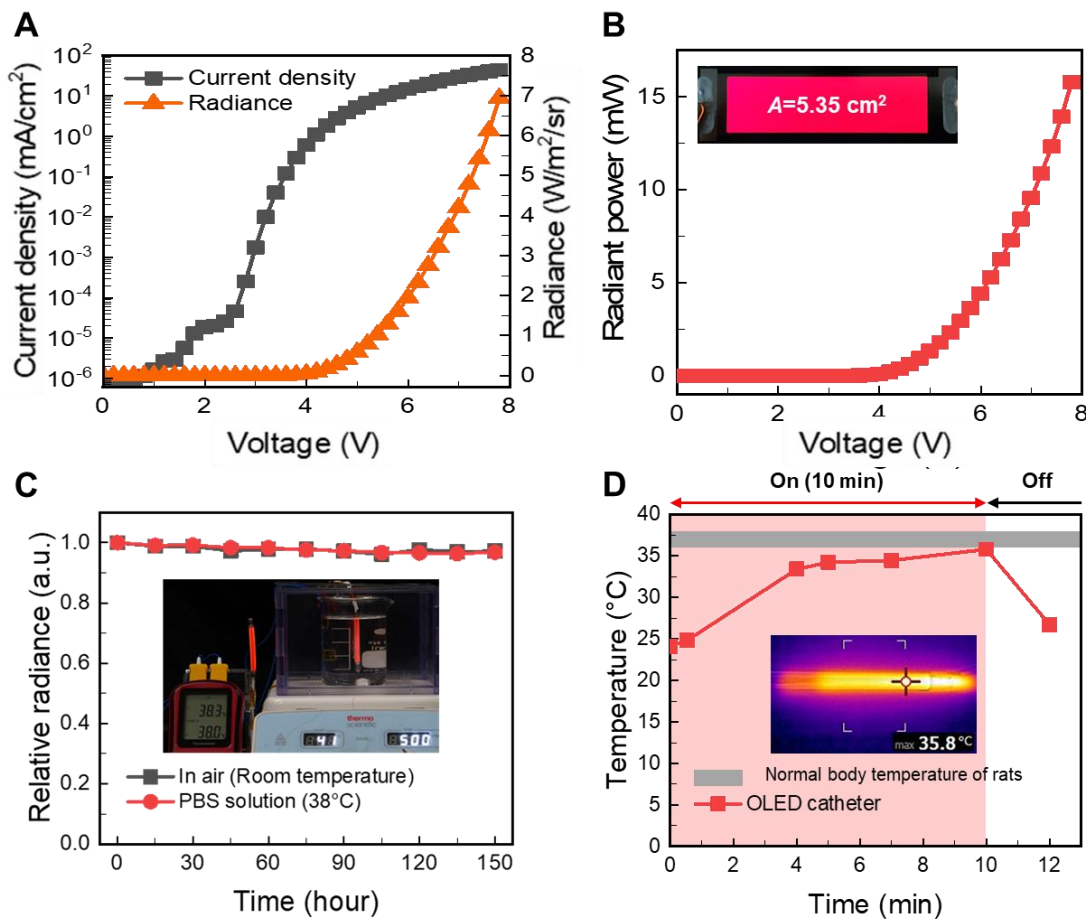
Figure 16 Characteristic of electrical, mechanical, and thermal stability proposed OLED catheter: **(A)** The current density (J) and radiance (R) of applied voltage (V), and **(B)** radiant power of applied voltage in OLED catheter. **(C)** Durability assessment of OLED catheter in PBS aqueous solution for an hour. **(D)** Thermal performance of the OLED catheter for 10 minutes.

We performed a laparotomy with small duodenal incision on the anesthetized GK rat and inserted an OLED catheter from the beginning of the duodenum. The median procedure time including anesthesia, incision of the abdominal wall, a small incision of the duodenum for the introduction of an OLED catheter, closure of the duodenal incision, and closure of the abdominal wall was 35 min (IQR: 31.75–36.50).

DMR with OLED catheter treated diabetic GK rats showed better glucose tolerance compared to sham control group, as shown lower glucose level at 15- and 30-min time points after 1 week and 30-min time point after 4 weeks (Figure 17B, $P < 0.05$). The areas under the curve in sham control group tended to increase after 1 week (+6.86%) and 4 weeks (+10.42%) without statistical significances (Figure 17C, left); however, the areas under the curve in OLED group showed a tendency to decrease after 1 week (–3.54%) and 4 weeks (–9.12%) of DMR with OLED without statistical significances (Figure 17C, right). Although there was no statistically significant difference in time within each group, there was a statistically significant difference between control and OLED group after 4 weeks of treatment (Figure 17D).
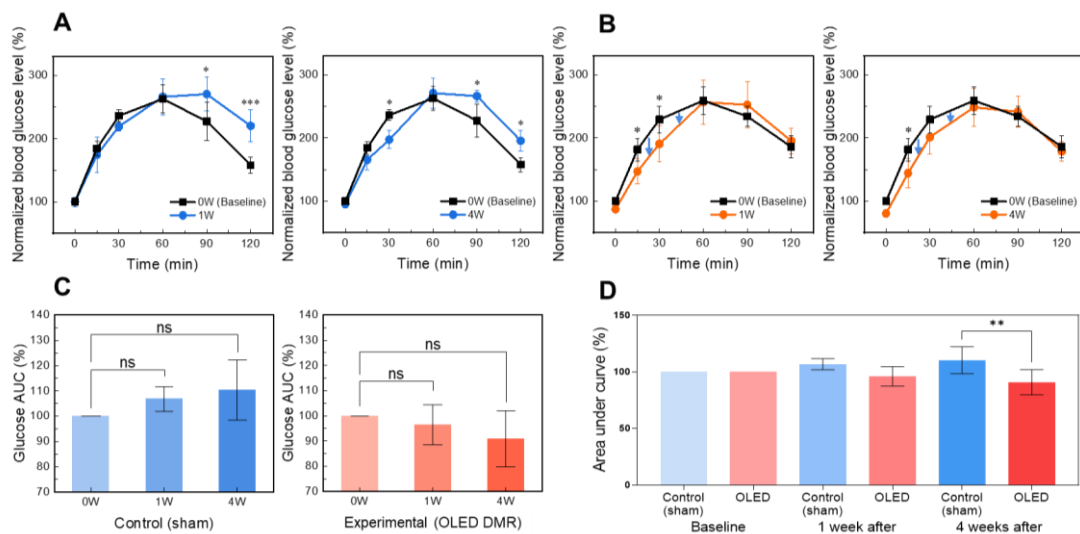
Figure 3 Glycemic curve during OGTT and normalized AUC in **(A)** control sham and **(B)** duodenal mucosal regeneration with OLED showing baseline, 1 week and 4 weeks after.

The GK rats are spontaneously diabetic model of non-insulin-dependent diabetes mellitus characterized by loss of β cells in the pancreatic islet, which is observed in sham

control group. Relatively preserved the pancreatic islets at 4 weeks after DMR with OLED were observed. The percentage of insulin-stained islet area in pancreatic section were greater (0.73 % vs. 0.48%) in DMR with OLED group in comparison with sham control group without statistical significance (Figure 18A). In accordance with histological liver section of Masson's trichrome (MT) staining, the percentage of collagen deposition in DMR with OLED was statistically lower (0.04 % vs. 0.14 %, $P < 0.001$) than that on the sham control (Figure 18B)
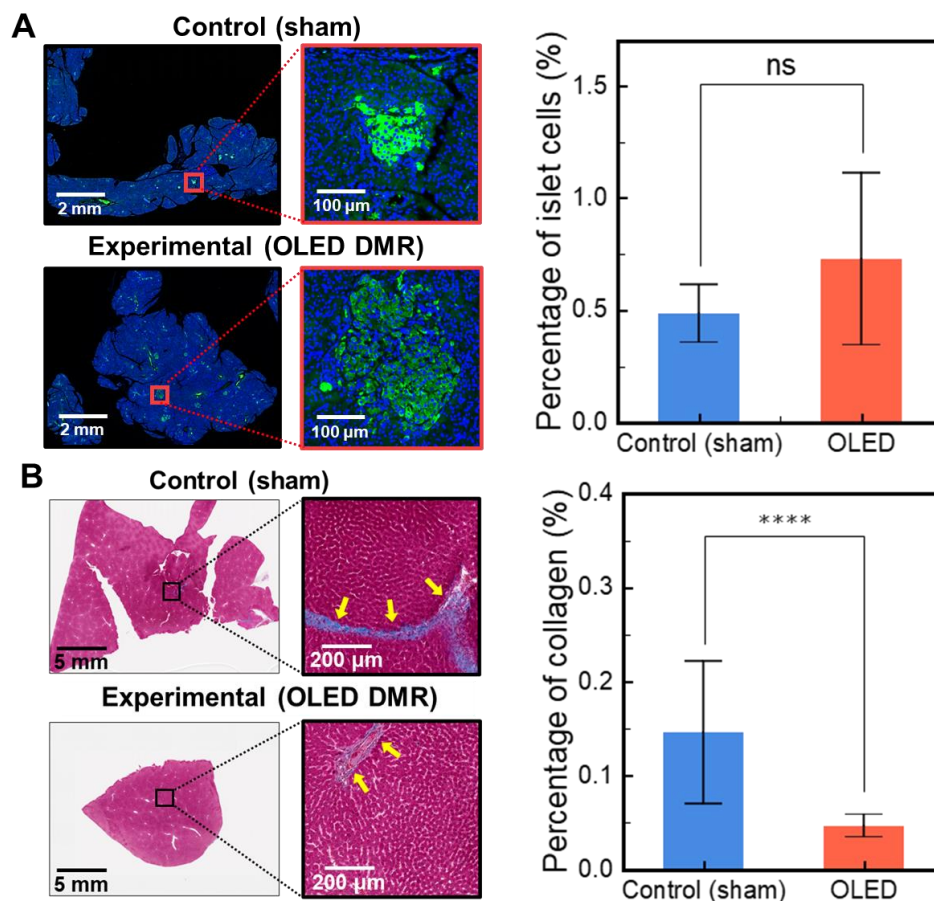
Figure 4 (A) Representative histopathological images (Masson's Trichrome staining) of liver section from sham control (upper) and the case-OLED group (below). Comparison of quantitative percentage of collagen deposition from the liver sections between sham control and case-OLED groups. **(B)** Representative pancreatic islets stained with immunohistochemistry for insulin from sham control (upper) and the case-OLED group (below). Comparison of quantitative percentage of total area with

insulin target stained in pancreatic section at the 4 weeks after DMR.

Insulin resistance, which was measured by homeostasis model assessment-insulin resistance (HOMA-IR) [62], significantly decreased ($P < 0.005$) at 1 week after of OLED DMR as well as the level maintained significantly low ($P < 0.05$) until 4 weeks. On the other hand, the insulin resistance of sham control group temporary decreased ($P < 0.01$) after 1 week and not maintained until 4 weeks after (Figure 19A). Additionally, treatment with OLED significantly reduced the cholesterol level after 4 weeks of post-treatment compared with after 1 week (63.98 mg/dL vs. 80.42 mg/dL, $P < 0.01$), which were shown increased (91.85 mg/dL vs. 74.45 mg/dL, $P < 0.01$) in sham control group after 4 weeks (Figure 19B). We also measured GLP-1 released at baseline, 1- and 4-week after DMR, GLP-1 AUC showed significantly decreased ($P < 0.05$) 1 week after compared with baseline and increased ($P < 0.01$) 4 weeks after compared with 1 week after DMR (Figure 19C). As shown in the sham control ($P < 0.01$) and OLED ($P < 0.005$) group results, we found that significantly decrease in insulin secretion after 1 week compared to baseline. However, significant increase in serum insulin level in 4-week compared to 1-week was observed in OLED group ($P < 0.01$) and not in sham group. (Figure 19D) For assessment of general health during experiment, we measured body weight and food intake at 3-day intervals. Food intake significantly decreased compared to the control group starting from day 12 post-DMR treatment. In contrast, body weight increased similarly in both groups. (Figure 20) In additions, no definite mucosal abnormality

or duodenal wall injury was seen in the OLED group. (Figure 21, Table 4)
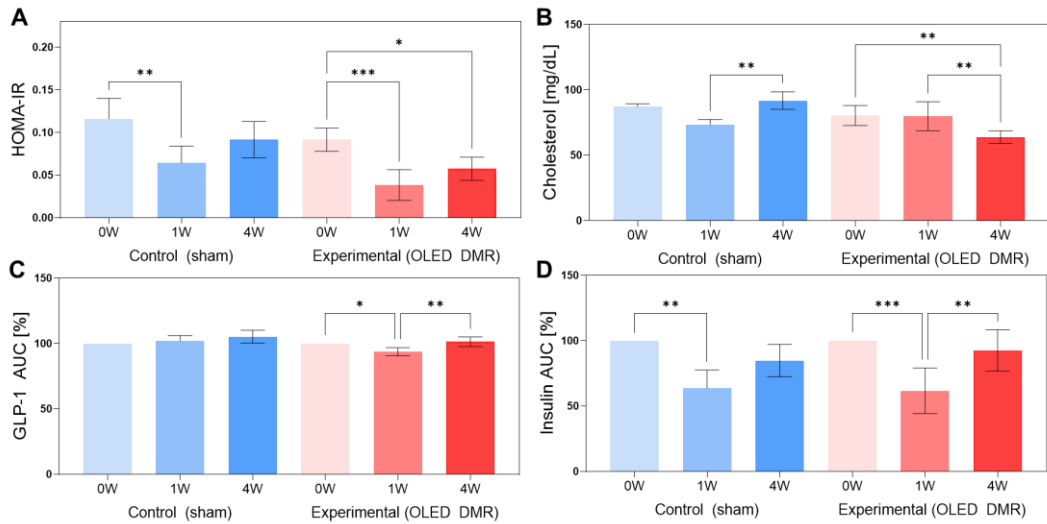
Figure 5 Comparison of **(A)** HOMA-IR and **(B)** cholesterol level in sham control and case-OLED group showing baseline, 1- and 4-week after DMR**.** Normalized the area under the curve for **(C)** GLP-1 and **(D)** insulin during OGTT in sham control and OLED group between baseline, 1- and 4-week after DMR. The data are presented as the mean ± SEM. ANOVA with the Bonferroni's post hoc test was used for statistical analysis. * $p < 0.05$, ** $p < 0.01$
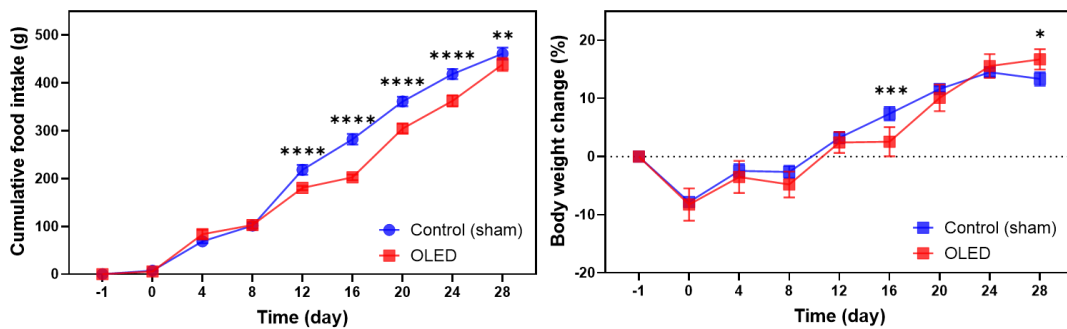
Figure 6 Comparison of the cumulative food intake (left) and body weight change between sham control (black line) and OLED group (orange line). During the observation period, food intake and body weight were measured through 9-monitoring session at intervals of 4 days including baseline (a day before DMR).
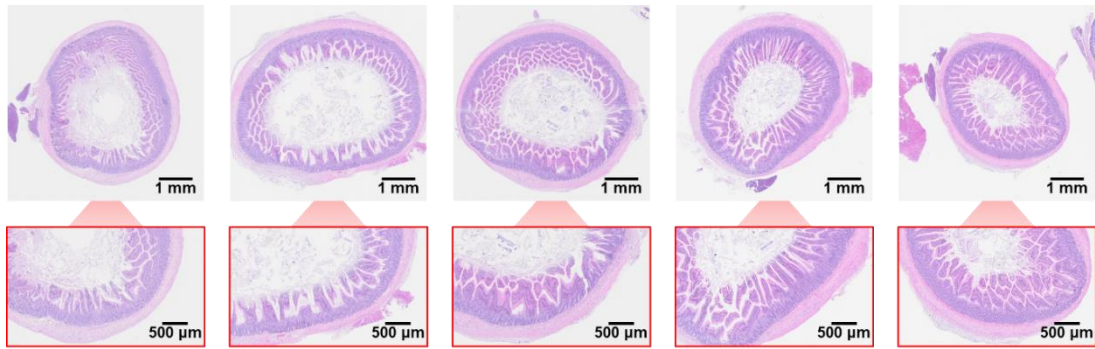
Figure 21 Representative histopathological images (stained with hematoxylin and eosin) of duodenum sections from the group treated with DMR using OLED catheter demonstrated granulomatous formation and mild ulceration in all sections, but no perforation was observed at the DMR treatment sites.

Score, mean ± SD	OLED	Control (sham)	P value
Inflammation	0.80 ± 0.75	0.60 ± 0.80	0.92
Necrosis	0	0	> 0.99
Congestion	0.20 ± 0.40	0	> 0.99
Neovascularization	0	0	> 0.99
Fibrosis	0.20 ± 0.40	0.80 ± 1.17	0.72
Mucosal hyperplasia	0.80 ± 0.75	0.60 ± 0.49	> 0.99
Total score	2.00 ± 1.10	2.00 ± 1.26	0.86

Table 4 Histopathological evaluations of the duodenal mucosa in GK rats were performed, with scores assigned for inflammation, necrosis, congestion, neovascularization, fibrosis, and mucosal hyperplasia. These were rated on a scale from 0 to 4, where 0 indicates no significant findings, 1 minimal, 2 mild, 3 moderate, and 4 severe. The results are expressed as mean ± SD. An unpaired t-test was used for statistical comparisons.

We observed changes in the gut microbiome composition in the OLED group 1 week after OLED DMR. The Firmicutes/Bacteroidetes ratio at the phylum level decreased by the 2nd week and increased from the 3rd week in the OLED group, while the ratio remained constant in the control group. At the family level, Bacteroidetes such as *Muribaculaceae* and *Bacteroidaceae* increased by the 2nd week after DMR (Figure 22A).

Using alpha diversity metrics, which represent species richness (Chao1, Simpson) and evenness (Shannon) in each sample, the OLED group showed different alpha-diversity analysis results compared to the sham control group (Figure 22B). Species diversity statistically increased after 2 weeks compared to baseline in the OLED group, with an increased Shannon index ($P < 0.05$) and a decreased Simpson index ($P < 0.05$). Additionally, beta diversity analysis, which measures significant differences between clusters using beta diversity distance, showed statistically significant differences at 1 week ($P < 0.05$) and 2 weeks ($P < 0.01$) after DMR compared to baseline (Figure 22C).

Based on these results, we identified significant changes in the gut microbiota at the genus level from baseline to 2 weeks after DMR, presented as a taxonomic bar-chart using LEfSe analysis. This method identifies specific microbiome biomarkers through the LDA score, measured by the difference in relative taxonomic composition (Figure 22D). Two genera (*Muribaculaceae_uc* and *Escherichia*) were significantly enriched after 2 weeks in the OLED DMR group ($P < 0.05$). In the sham control group, five genera (*Turicibacter, KE159605_g, Lactobacillaceae_uc, Sporobacter, Caproiciproducens*) were significantly enriched after 2 weeks ($P < 0.05$). Specifically, after 2 weeks, *Muribaculaceae_uc*, belonging to the family *Muribaculaceae*, was significantly enriched in the OLED group and reduced in the sham control group. In contrast, *Erysipelotrichacea_uc*, belonging to the family *Erysipelotrichaceae*, significantly reduced in the OLED group and was enriched in the sham control group compared to baseline.
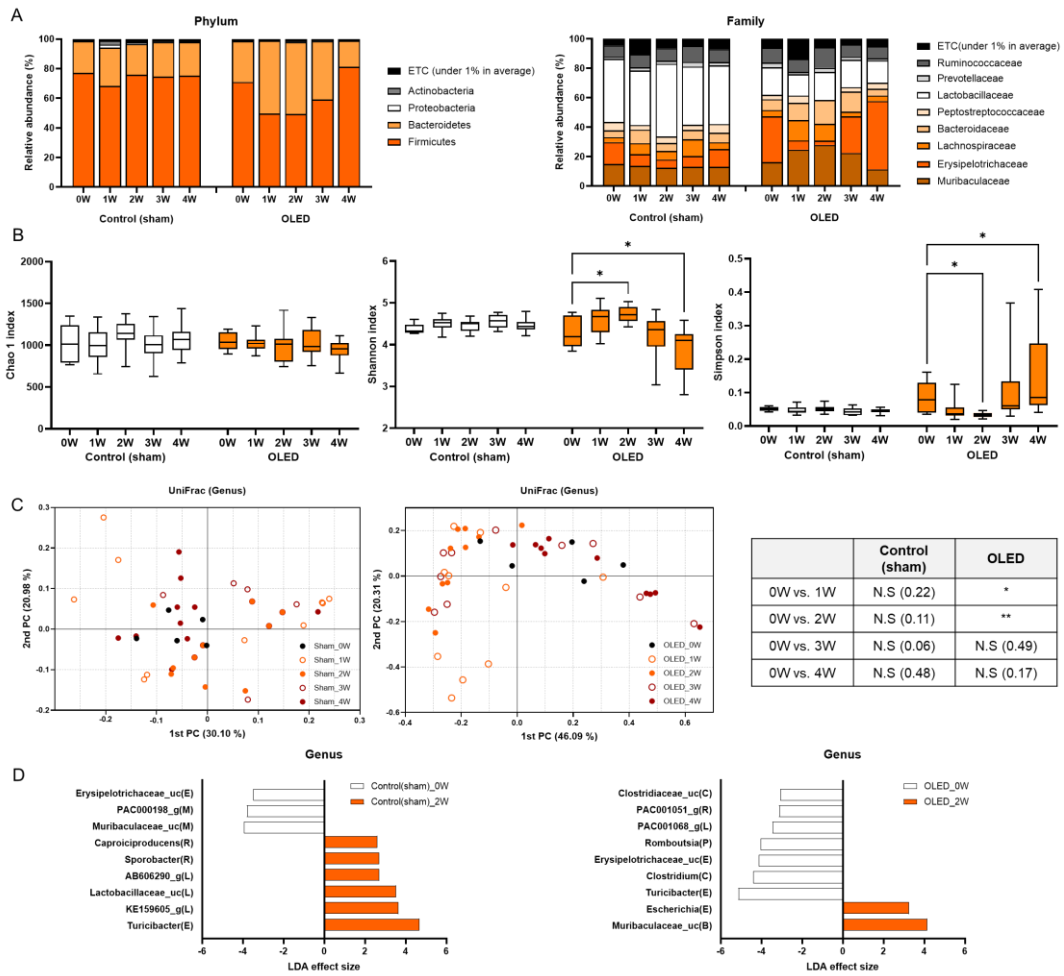
Figure 7 Comparison of gut microbiome after DMR. **(A)** Composition profiles of the gut microbiome at phylum and family level in sham control and OLED group at baseline, 1-, 2-, 3-, and 4-week after of DMR. **(B)** α diversity analysis: Chao1 index and Simpson index reflecting the richness and Shannon index reflecting evenness of diversity in gut microbiome. **(C)** β diversity analysis: Principal coordinate analysis (PCoA) plot using Unifrac distance of gut microbial communities obtained from two groups at 0-, 1-, 2-, 3-, and 4-week after of DMR **(D)** Differentially represented genus between 0- and 2-week in each group by linear discriminant analysis effect size (LEfSe)

3. Results from Experiment (3):

In actual clinical applications, the issue of heating is critically important. Therefore, before applying the device to patients, we designed a comprehensive protocol to evaluate the stability of the device by monitoring temperature changes not only in *ex vivo* but also in in vivo conditions through animal experiments. Firstly, we conducted *ex vivo* experiments involving using the liver and duodenum from pigs to evaluate the safety of endoscopic DMR application prior to preclinical *in vivo* study using mini pigs. Under various power mode (continuous mode of 720-second, intervals mode of 360-, 180-, 120-, and 60-second), we compared temperature from sensor attached to the endoscopic DMR application with those measured by an infrared thermometer (FLIR E6-XT, FLIR Systems) to validate accuracy of temperature sensor. Through this experiment, we observed that temperatures measured by the thermometer every 30 seconds was higher than those measured by the sensor, with average differences of 6.89°C (continuous mode: 720-sec), 1.2°C (interval mode: 360-sec), 2.36°C (interval mode: 90-sec), 0.27°C (interval mode: 90-sec), and 1.63°C (interval mode: 60-sec). Except for the continuous mode (720-sec), temperature differences between the sensor and thermometer reader were within 3 °C. The highest temperatures recorded before the end of the experiment were 61.8°C (continuous mode: 720-sec), 57.4°C (continuous mode: 720-sec), 54°C (interval mode: 90-sec), 50.3°C (interval mode: 90-sec), and 48.7°C (interval mode: 60-sec). (Figure 23)
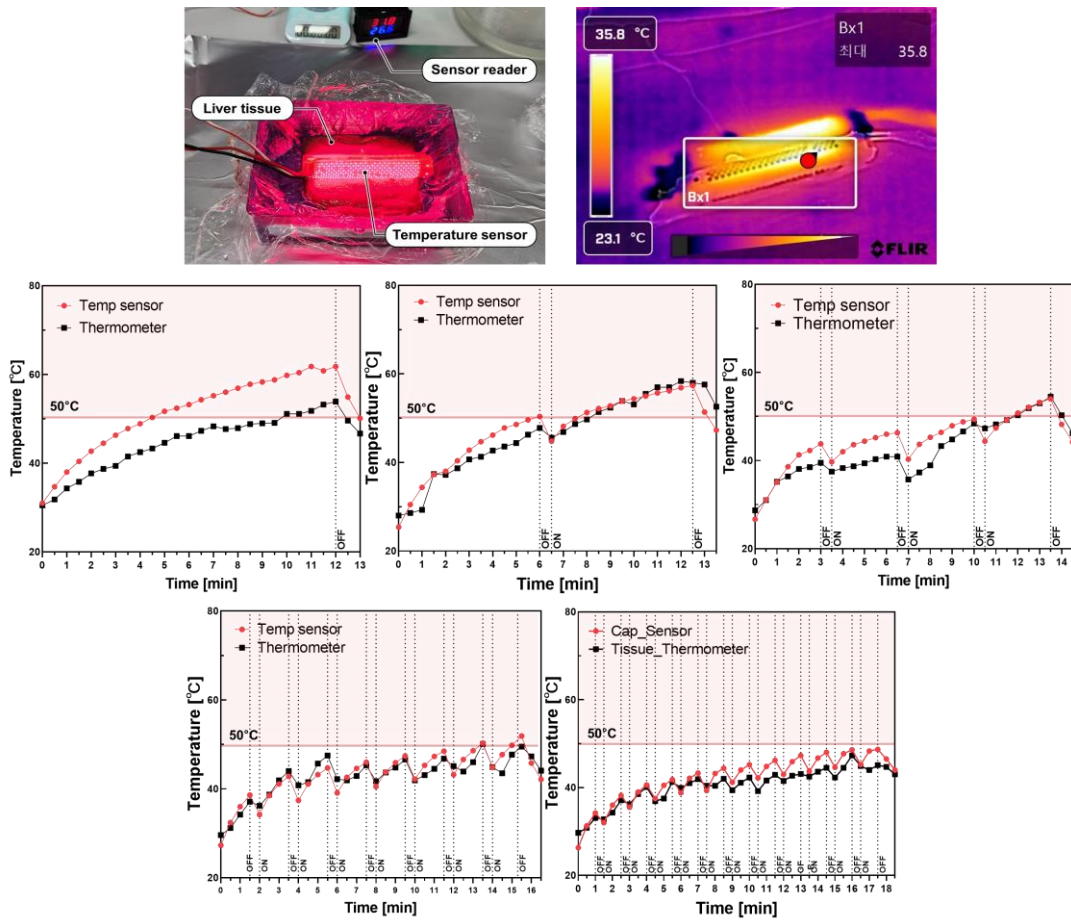
Figure 8 Comparison of temperatures measured by the temperature sensor equipped in endoscopic DMR application and the infrared camera under various power mode.

To perform DMR procedures under *in vivo* conditions in the mini pig model, we set the DMR energy at 90-sec interval mode to maintain temperatures below 50°C based on ex vivo experiments. To compare the temperature between *in vivo* and *ex vivo* systems at same power mode (interval mode: 90 sec), we measured the temperature values by sensors during DMR procedures in mini pigs with those measured values by sensor in the ex vivo experiment using duodenal tissue of pigs. Although each initial temperature was not matched ($T_{ex\ vivo}$ = 27.3 °C, $T_{in\ vivo}$ = 37.8 °C), the temperature between ex vivo and in vivo became similar within about 1°C by the end of the DMR procedure. (Figure 24).
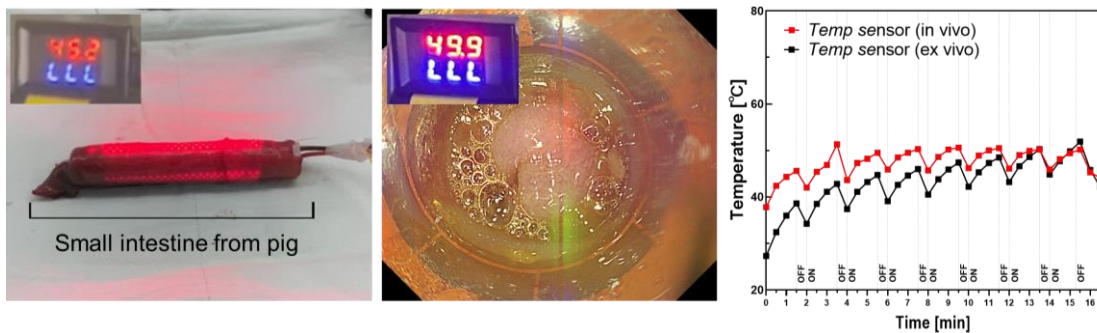
Figure 9 Comparison of temperature measured under *ex vivo* and *in vivo* condition during DMR procedure of 90-sec interval mode.

Mean procedure time including introducing endoscopy to first portion of duodenum, operating endoscopic DMR application (15 minutes 30 seconds) and capture treatment lesion and closure for DMR application was 31 minutes (IQR: 21-37). After one week of DMR procedure, we performed surveillance endoscopy to evaluate the treated duodenum mucosal area for injury such as erythema, ulceration, or hemorrhage. We could not observe any adverse event and secondary complication in the treated lesion. (Figure 25)
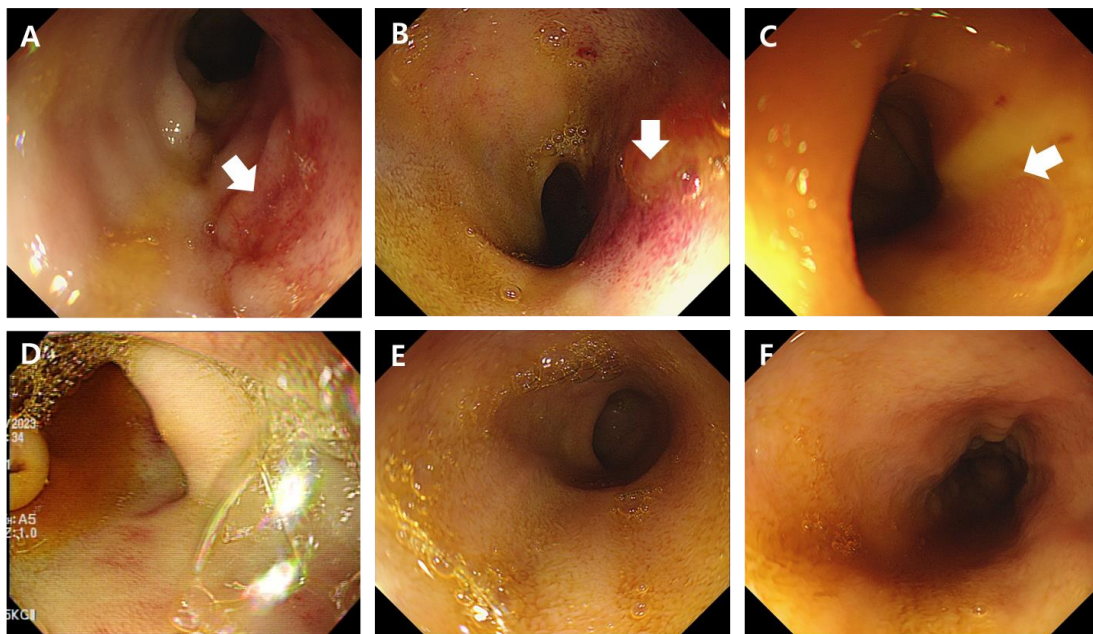
Figure 10 Endoscopic images immediately after DMR (A, B, C) and after one week of recovery (D, E, F) from experiment group (n = 3) The arrow indicates slight mucosal damage occurred after DMR.

Endoscopic DMR application equipped with mini LED chips of 630 and 850nm wavelength was used to treat type 2 diabetic mini pig model. (n=3, 9-14 months, 33.86kg) In this experiment, fasting blood glucose was measured at every 3 days. It was observed that fasting blood glucose significantly decreased by 40.78% (P<0.001) after DMR compared to baseline. (Figure 26A) When interpreting weekly observation points, a significant reduction of 37.84% (P < 0.01) in fasting blood was observed after 2 weeks after DMR treatment compared to baseline. Additionally, at the end of the observation period, 6 weeks post-procedure, fasting blood glucose was found to have decreased by 66.76%. (Figure 26B)
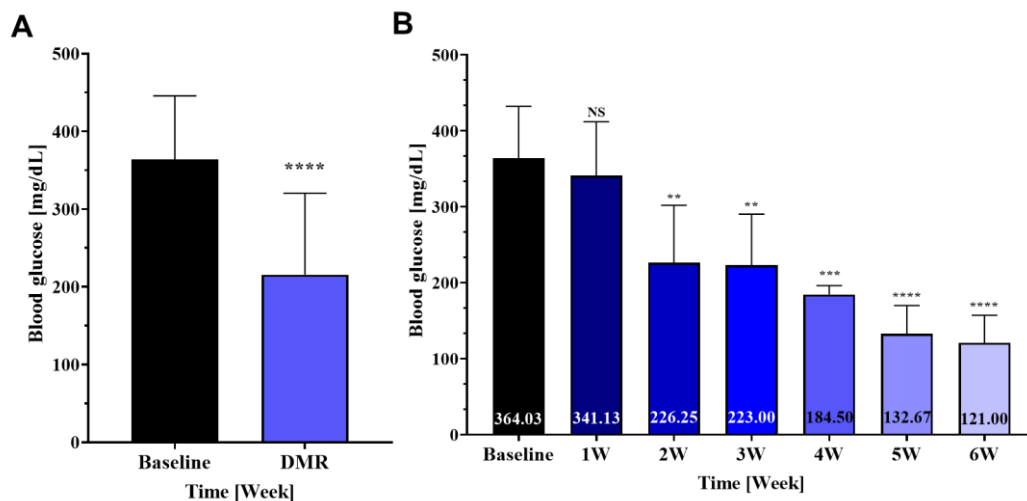
Figure 26 Changes in fasting blood sugar (FBS) levels in type 2 diabetic minipigs after DMR treatment: comparing FBS **(A)** pre and post DMR, as well as **(B)** on a weekly basis.

Type 2 diabetic mini pigs showed better glucose tolerance compared to sham control group, as shown lower glucose level at 0- ($P < 0.05$), 30- ($P < 0.01$) and 60-min ($P < 0.05$) time points after 2 weeks. (Figure 27B) At the 5-week of post DMR, the glycemic curve decreased at 0- ($P < 0.01$), 15- ($P < 0.05$), 30- ($P < 0.005$), 45- ($P < 0.01$), 60- ($P < 0.005$), 90-

($P < 0.05$) 120- ($P < 0.05$), 150- ($P < 0.01$) and 180-min ($P < 0.05$). (Figure 27C) The areas

under the curve in DMR treated showed a tendency to decrease after 1 week (–33.57%) and 4

weeks (–32.5%) of with dual wavelength without statistical significances, while there was a

statistically significant 28.27% decreased in glucose AUC at 5 week of post DMR. (Figure

27D)
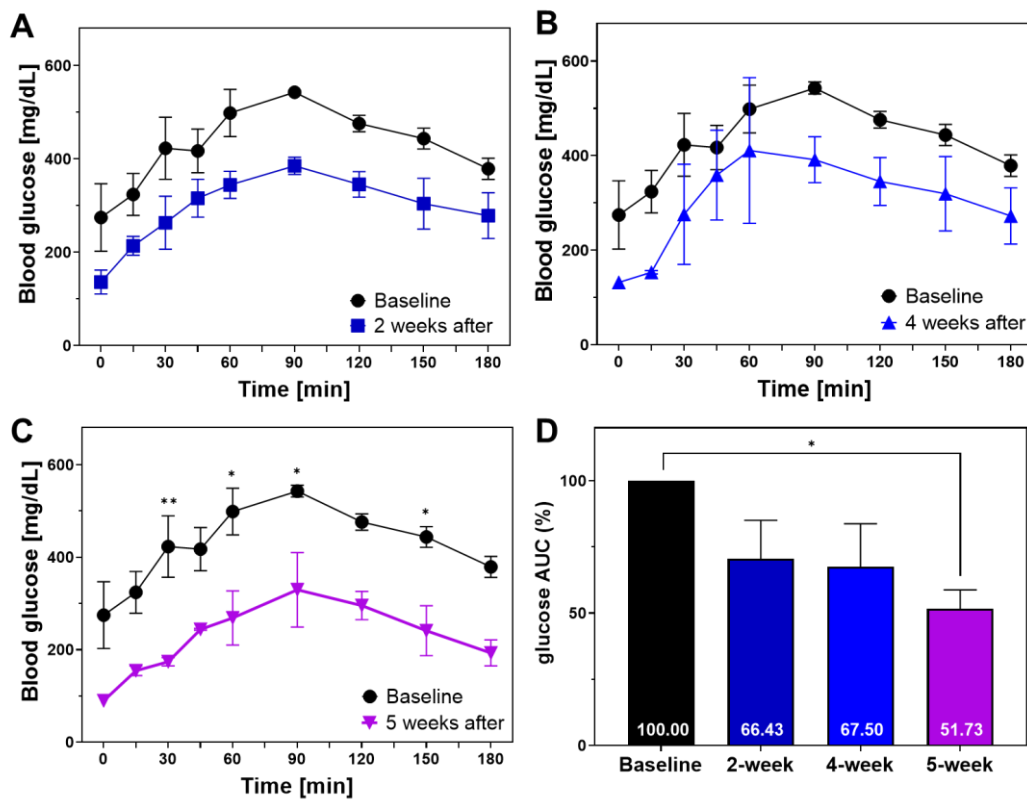
Figure 27 Glycemic curve during oral glucose tolerance test (OGTT) and normalized area under curve

in comparison of baseline, 2-, 4- and 5-week after DMR using endoscopic DMR application in type 2

diabetic minipig model (n=3).
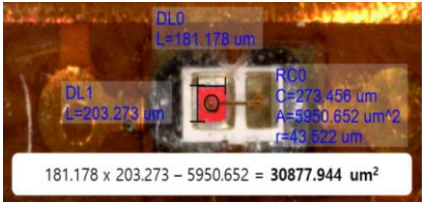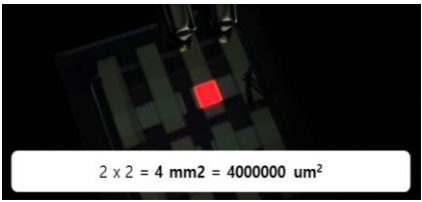
DISCUSSION

1. Bridging DMR application with LED and OLED technologies

In this study, we investigated the effects of DMR using three different applications. Firstly, we examined the effects of DMR using an LED catheter. This study aimed to determine the optimal light output and wavelength conditions, maintaining a temperature below 50°C. The results demonstrated the therapeutic effects of the point light source, validating the treatment efficacy based on output energy and wavelength.

(1) **LED catheter vs. OLED catheter:** In the second experiment, we evaluated the DMR effects using an OLED catheter application, which provides uniform mucosal stimulation and high thermal efficiency compared to the LED catheter application conditions. In the experiments using the LED catheter and the OLED catheter, the output power (LED: 1.40 mW, OLED: 1.57 mW) was set to the same value and used as a fixed variable. (Table 5) Using a photodiode and spectrometer, we measured the power of a single LED (approximately 0.07 mW), and for a dual-sided catheter with 20 LEDs, the total light output was approximately 1.40 mW (Figure 8). For the OLED catheter, we calculated the power based on the J-V-L curve a vcfdxnd angular spectrum data, estimating a total output of about 1.57 mW at 4.8V (Figure 16), considering the surface area of the cylindrical OLED catheter. Consequently, second experiment using OLED catheter assessed the DMR effect, focusing on uniform light distribution and efficient light stimulation minimized heating effect, comparable to the total power LED catheter in first experiment.
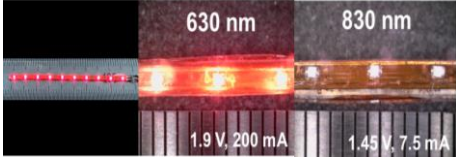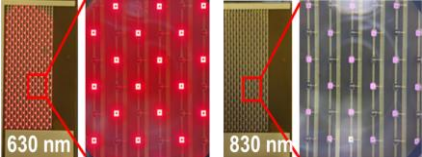
	Catheter light source type	
	LED (point light source)	**OLED (surface light source)**
Unit device	181.178 x 203.273 − 5950.652 = **30877.944** um²	2 x 2 = 4 mm2 = **4000000** um²
Power of unit (O)LED	0.07 mW	0.01 mW
Power density of unit (O)LED	234 mW/cm²	0.29 mW/cm²
Total Power of catheter	1.40 mW	1.57 mW

Table 5 Comparison of optical properties between LED catheter and OLED catheter used in preclinical studies with rat model

(2) **LED catheter for rat model vs. LED endoscopic DMR application for pig model**: The third experiment aimed to develop a device for clinical applications by scaling up the dual-wavelength LED catheter used in GK rat model to be applicable in diabetic minipig model. During the scaling process from the rat model to the mini pig model, adjusting the irradiation dosage was an important issue. Therefore, we accounted for physiological differences such as the duodenal diameter between rat and mini-pig models. Assuming a scale-up from the average rat duodenum diameter of 2.5 mm [63] to the mini pig duodenum diameter of 2.5 cm [64], we increased the area by 100 times (based on the square of the diameter), adjusting the energy density accordingly. Since the pitch between the LED chips designed for the LED catheter and the endoscopic LED DMR application differs, the light intensity measurement for scale-up was performed by comparing the output of the devices measured by a 1cm x 1cm sensor of

the power meter, rather than comparing the light output of a single chip. Additionally, for the LED endoscopic DMR application intended for clinical settings, it was essential to design a power mode within a safe range to address thermal issues under maintaining same input irradiation conditions (Table 6). Therefore, based on *ex vivo* experiments, we selected an on-off power mode that did not exceed the critical temperature of 50°C, which causes tissue necrosis, with an on-off duration of 1 minute 30 seconds. (Figure 23)

	Catheter light source type	
	LED catheter application	**LED endoscopic application**
Unit device		
Number of LED chips	20 (630nm), 20 (850nm)	473 (630nm), 473 (850nm)
LED pitch	5 mm (630-630nm/850-850nm) 2mm (630-850nm)	3 mm (630-630nm/850-850nm) 1.5 mm (630-850nm)
Diameter of target organ	0.25 cm	2.5 cm
Surface of catheter	2 cm2	22.4 cm2
Power density	11.4 mW/cm^2	114.2 mW/cm^2
Total Power of catheter	22.8 Mw	2553.6 mW

Table 6 Comparison of optical properties between LED catheter used for rat model and LED endoscopic DMR application used for mini pig model

2. Promising outcomes of DMR with LED/OLED catheter in treating T2DM

Our research was focused on evaluating the efficacy of DMR using red or infrared LED light in a T2DM animal model as a non-pharmacological treatment approach. The study demonstrated that DMR with LED resulted in improvements in serum glucose levels and hepatic parameters, and these effects were sustained during the 4-week follow-up period in GK rats following a single session of DMR.

Additionally, the study on DMR with an OLED catheter demonstrated promising results in the treatment of T2DM. The DMR using OLED group exhibited a notable reduction of about 9.1% in the AUC of blood glucose levels after 4 weeks compared to the sham control group. Furthermore, this group effectively lowered HOMA-IR levels, indicating improved insulin sensitivity. These positive effects were sustained even after 4 weeks of DMR, implying that a single session of duodenal DMR with an OLED catheter could have a lasting impact on reducing insulin resistance.

Moreover, the DMR using LED/OLED light group showed a significant decrease in the collagen ratio in the liver compared to the control group, suggesting a reduction in liver fibrosis. These findings suggest that DMR with the LED/OLED catheter directly influenced the duodenal mucosal of GK rats, leading to improvements in T2DM and liver fibrosis, along with consistent alterations in various metabolic parameters. These pilot studies underscore the potential of DMR using OLED light as a therapeutic approach for addressing not only T2DM but also related complications such as liver fibrosis.

3. Potential and mechanisms of DMR using LED/OLED catheters for T2DM

There is existing evidence to support the use of DMR using LED/OLED catheters as a safe and effective phototherapy for individuals with diabetic complications. Previous animal studies have shown that external PBM using LED chips applied to the pancreas in streptozotocin-induced diabetic rodent models led to increased cell density in islets and pancreatic ducts, promoted hepatic glycogenesis, and altered carbohydrate metabolism. [45, 46] Additionally, findings from an ex vivo study suggest that external irradiation of infrared light using LED could impact insulin secretion in the pancreas, even when not specifically targeted at the pancreas, indicating the potential therapeutic effects of DMR using LED catheters in diabetes management. [51]

To date, an optimal LED wavelength for DMR has not been definitively established. Typically, wavelengths around 600 nm or 800 nm are commonly used for external PBM in animal models (Table 1). Studies have investigated the combined use of light at 600 nm and 800 nm wavelengths due to their distinct cellular signaling and tissue penetration capabilities. In a 1-week follow-up and subsequent 4-week follow-up study, DMR using a dual wavelength LED catheter demonstrated consistent efficacy in reducing serum glucose levels compared to DMR sessions using a single wavelength catheter. The combination of 630 nm and 850 nm DMR using LED light may have distinct roles in modulating the gut microbiome and insulin resistance. Following 630 nm DMR, there could be alterations in the gut microbiome and improved insulin sensitivity, leading to increased insulin expression in pancreatic islet cells

and higher serum insulin levels over a 1 to 4-week period after DMR with 850 nm light. This strategy of utilizing multiple wavelengths of LED light shows promise in enhancing serum glucose levels and hepatic parameters by effectively penetrating from the duodenum to the pancreatic parenchyma. Further assessment of the diverse therapeutic potential of DMR with multi-wavelength compared to DMR with single wavelength is necessary to fully understand and harness the benefits of this combined approach for metabolic disorders. Additional studies are warranted to explore the specific mechanisms and outcomes associated with the utilization of various wavelengths in LED light therapy for improved glucose regulation and liver function.

Our findings demonstrated a significant decrease in the AUC of blood glucose levels during the OGTT even after DMR with a single wavelength, lasting up to 4 weeks compared to the baseline. Notably, serum insulin levels during OGTT increased, while HOMA-IR decreased following DMR with dual wavelength, indicating enhanced insulin secretion coupled with reduced insulin resistance. Moreover, pancreatic islets in the DMR with dual wavelength group exhibited better preservation compared to the control group, suggesting possible beta-cell regeneration and enhanced insulin secretion mediated by duodenal enteroendocrine cell stimulation and increased endogenous gut hormone release regulating glucose homeostasis. Elevated serum levels of GLP-1 and insulin at 4 weeks compared to 1 week post-DMR with dual wavelength suggest an enhancement in glucose-mediated insulin secretion by GLP-1. However, there was no observable difference in serum levels of GIP post-

treatment. The exact mechanism through which DMR with dual wavelength influences proliferating β-cells in the pancreas, either directly or indirectly by modulating other gut hormone levels, requires further investigation for a clearer understanding.

Furthermore, DMR with dual wavelength may aid in reducing insulin resistance through mechanisms similar to those observed in metabolic improvements post Roux-en-Y gastric bypass surgery. These mechanisms may involve reductions in hepatic glucose production, alterations in bile acid metabolism, attenuation of metabolic endotoxemia via reduced intestinal permeability, and modifications in host-microbial interactions. The durable effect of lowering serum glucose levels over 4 weeks with a single DMR with dual wavelength light session at a lower power density compared to multiple higher power density sessions of extra-body PBM with LED chips in earlier animal studies suggests the duodenum as a key therapeutic target in metabolic diseases like T2DM.

The 4-week follow-up group utilizing 4-dimensional LED with higher energy intensity compared to the 1-week pilot study displayed a slight increase in the reduction of glucose levels during the OGTT, indicating that consistent irradiation at an optimal energy intensity in DMR using LED light may impact the degree of lowering serum glucose levels.

4. Gut microbiome alterations following DMR using LED/OLED catheter

One noteworthy discovery from this study is the observed alteration in the gut microbiome following DMR with dual wavelength. In the DMR group, specific genera such as Bacteroides, Escherichia, Parabacteroides, Allobaculum, and Faecalibaculum were significantly enriched after 1 week, with a notable increase in Bacteroides *acidifaciens*. Conversely, five genera from the *Lachnospiraceae* family significantly decreased after 1 week, indicating a shift in the gut microbiome. Previous studies have shown that infrared wavelength PBM can increase *Allobaculum*, a bacterium associated with a healthy microbiome, similar to the findings in this study. [65] Despite no observed enhanced expression of GIP and GLP-1 in the duodenal mucosa after 4 weeks following DMR with dual wavelength, the alteration of the gut microbiome from 1 week to 4 weeks post-DMR, along with changes in serum GLP-1, insulin levels, and improved insulin resistance as indicated by HOMA-IR, suggests that DMR with dual wavelength may directly impact gut microbiome alteration, leading to decreased serum glucose levels. The reduction of AUC in the DMR with dual wavelength group at 4 weeks in the 4-week follow-up study was greater than that observed at 1 week, indicating that the dynamic alteration of the gut microbiome following DMR with dual wavelength might contribute to the sustained reduction in serum glucose levels.

Bacteroides *acidifaciens*, known for its association with weight and fat loss and improved insulin sensitivity, increased post-DMR with dual wavelength, aligning with its potential role in influencing serum glucose changes. [66] The observed alterations in gut

microbiome composition, including the increase in Allobaculum and Bacteroides acidifaciens while decreasing Lachnospiraceae, have significant implications for reducing serum glucose levels and addressing hyperglycemia. These findings indicate that the modulation of the gut microbiome induced by duodenal mucosa resection using LED light could play a pivotal role in enhancing metabolic outcomes and regulating glucose levels. [67]

It is widely recognized that T2DM and non-alcoholic fatty liver disease (NAFLD) are intricately connected through insulin resistance as a common underlying pathological mechanism. These two metabolic conditions often coexist in individuals. While our study utilized GK rats, a non-obese model of T2DM, and did not track changes in body weight or liver fat content during the 4-week follow-up period, our findings did reveal a decrease in liver enzymes such as AST and ALT following DMR with dual wavelength. This suggests an additional favorable effect of DMR on concurrent NAFLD, highlighting the potential benefits of DMR with LED light therapy in addressing both T2DM and associated liver conditions like NAFLD.

Following the findings mentioned earlier, the DMR study using an OLED catheter also confirmed similar results of gut microbiome alteration. The enrichment of the Muribaculaceae family observed after 2 weeks in the DMR using OLED catheter group may be significant due to the abundant enzymes within this family that aid in decomposing complex carbohydrates and proteins. [68] This family is closely linked to diabetes treatment mechanisms. In addition, the enrichment of the Erysipelotrichaceae family noted after 2 weeks

in the sham control group may potentially contribute to gut inflammation and could be a microbial target of interest for managing metabolic disorders, including T2DM. [68, 69] Furthermore, the decrease in the Firmicutes/Bacteroidetes ratio in the OLED group 1-2 weeks post-DMR could be associated with an increase in glucagon-like peptide-1 (GLP-1) secretion, possibly due to the presence of gut microbial species that produce short-chain fatty acids. The results suggest that DMR with OLED may impact the gut microbiome, leading to dynamic changes in serum GLP-1 and insulin levels at 1 and 4 weeks. This indicates that alterations in the gut microbiome following DMR could have a delayed effect on the onset of treatment for hyperglycemia and insulin resistance. Previous research has shown that the use of duodenal or external PBM in small animal models resulted in similar delayed alterations of the gut microbiome after 1-2 weeks of DMR, supporting the findings of the current study. Therefore, considering the observed changes in the gut microbiome, fluctuations in serum GLP-1 and insulin levels, and improved insulin resistance as demonstrated by the HOMA-IR from 1 week to 4 weeks in the OLED group, it is suggested that DMR with OLED light may influence the abundance of gut microbial species producing short-chain fatty acids, leading to reduced serum glucose levels and insulin resistance through increased GLP-1 production.

Although our results of the gut microbiome indicated a correlation between DMR procedures and alteration of gut microbiome, it remains unclear whether the observed results are causative factors in the pathophysiology of diabetes or secondary phenomena. To validate these findings, it is necessary to conduct mechanistic studies such as specific fecal microbiota

transplantation (FMT). This approach will help elucidate how microbes interact with the host, induce immune responses, and produce metabolic byproducts.

5. *High potential for real-world medical device implementation*

While existing DMR devices like Revita and ReCET as mentioned in introduction paragraph provide valuable treatment options, there are several limitations that need to be addressed to improve their efficacy, safety, and accessibility. First, DMR procedure using existing device can vary in technical complexity depending on operator skill or patients' anatomy, leading to variability in outcomes. Due to irreversible therapy way, there is a potential risk of complications such as perforation, bleeding, or infection if the procedure is not performed correctly. According to the literatures [41], the average duration of conventional DMR procedure is approximately 60 minutes, relatively time-consuming process. On the other hand, through our newly developed endoscopic DMR application, we observed an improvement in blood glucose levels in the diabetes model. Moreover, we confirmed that there was no mucosal damage after DMR which is not over 50 °C as well as the procedure did not require any extra manipulation, resulting in a reduced average procedure time (mean duration: 31 minutes). Through experiment conducted on diabetic mini pig, we have demonstrated the safety, functionality, and feasibility of the developed endoscopic DMR application with mini-LED chips in this study.

6. Key observations from interconnected DMR experiments

Based on experiments conducted under various conditions, we propose the following observations.

(1) Preservation of Pancreatic Islets with 850 nm wavelength light: Experiments using the dual-wavelength LED catheter showed preservation of pancreatic islets following DMR treatment. In contrast, while there was a trend of increase with the single-wavelength OLED DMR treatment (600-700 nm range), it was not significantly effective. The 850 nm wavelength, which has a longer penetration depth (5-10mm) compared to the 630 nm wavelength (approximately 3mm), likely promotes regeneration of the pancreas located deeper within the body.

(2) Significant Changes in Gut Microbiome with 600-700nm wavelength of OLED: Significant changes in gut microbiome clusters were observed after DMR treatment with a single-wavelength OLED (600-700nm range) light source, which does not produce heat, compared to the dual-wavelength (630/850nm) point-source LED catheter. The red light within 600-700 nm induced changes in the gut microbiota, leading to a reduction in blood glucose levels. This suggests that changes in gut microbiota can be triggered by specific wavelength light stimulation rather than thermal effect.

(3) Better improvement in hyperglycemia using endoscopic DMR application for pig: Significant reduction in blood glucose levels was observed in the dual-wavelength LED experiments compared to the OLED catheter experiments. The endoscopic DMR application

developed for mini-pigs (946 chips) has more than ten times the light output per unit area (630: 17.82 mW/cm², 850: 97.04 mW/cm²) compared to the small animal LED catheter (40 chips). The increased number of LEDs resulted in enhanced therapeutic effects due to the heating effect and deeper tissue penetration of the 850nm wavelength light.

These observations highlight the potential advantages of using dual-wavelength LED catheters for deeper tissue penetration and effective gut microbiome modulation, which could lead to significant improvements in pancreatic function and blood glucose levels. Further research is necessary to optimize these findings for clinical applications.

7. Limitation

One significant limitation of our study is related to the observation period established for post-DMR treatment monitoring in preclinical trials using GK rat model. Specifically, the four-week observation period following DMR, which included laparotomy, might presents challenges in distinguishing between the treatment period from DMR and the recovery period from laparotomy. Given that both processes are occurring simultaneously within this timeframe, it becomes difficult to separate and accurately interpret their individual effects on the observed outcomes. In the context of experiments that involve invasive procedures such as laparotomy, it is imperative to consider a longer observation period than the four weeks utilized in this study. In the further study, we need to extend observation period for a more accurate assessment of the long-term efficacy and safety of the DMR.

Second limitation of our study involves the interpretation of the results within the context of diabetes pathophysiology. Also, it remains uncertain whether the observed outcomes are primary causative factors in the development of T2DM or merely secondary manifestation of the disease. In other words, it is challenging to determine whether the observed phenomena contribute directly to the pathogenesis of diabetes or if they are simply consequences of the disease process. Detailed mechanistic studies are essential to clarify the causal relationships and to better understand the role these factors play in the pathophysiology of diabetes. Therefore, it is recommended that subsequent studies prioritize the exploration of these mechanisms to establish clearer cause-and-effect relationships in the future study.

Although this pilot study primarily examined the impact of DMR on T2DM, its potential implications extend further. Future clinical studies could explore using inner-body DMR to treat various other conditions. The capability of DMR applications to irradiate the entire affected area symmetrically with uniform light intensity and minimal heat dissipation presents significant advantages. However, since this study utilized rats or mini-pig for animal models, there might be differences in therapeutic efficacy when applied to humans in clinical settings.

The STZ-induced diabetic pig model is commonly used in medical research to study metabolic disorders like diabetes. While STZ-induced diabetic pig model in our study has several advantages that cannot be achieved using rodent models such as similarity to human diabetes in terms of metabolic features, there are still limitations to consider. One of major

limitation of STZ induced diabetic pig model is low reproducibility that STZ administration results in variable levels of diabetes induction among individual pigs. Also, in comparison of human, some studies have reported that pigs may have lower level of GLUT2 expression which is crucial important protein involved in glucose uptake. [70, 71] It might lead to difficulties in proper glucose transport that impede the accurate simulation of glucose metabolism in diabetic models for reliability of diabetes research models. [72] To address these limitation, we have consistently fed the HFHS diet. Furthermore, in future studies, we plan to validate the model through STZ induced diabetic control group without DMR therapy.

Lastly, experiments using animal model emerged two notable limitations: (1) the apparent therapeutic effects in the control group and (2) individual variability within the experimental group.

(1) Control Group Effects: Occasionally, several outcomes in control groups may be exhibited signs of improvement that mimic therapeutic effects. This phenomenon can result from placebo-like effects, natural recovery, or design flaws in the study. [73, 74] To address this, future studies should implement blind experimental designs, utilize random allocation of subjects, and ensure sufficiently large sample sizes to mitigate natural recovery effects. Moreover, establishing a well-matched control group that mirrors the experimental conditions without the treatment intervention is crucial.

(2) Individual Variability in Experimental Groups: Variability among individuals within the experimental groups can arise from genetic diversity, environmental factors, and

differences in health status. To minimize these effects, future studies should consider using genetically homogeneous animal models, standardize environmental conditions, and select subjects with similar health statuses. [75] Increasing the sample size and conducting repeated experiments will also help ensure that the results are statistically significant and reproducible. [76, 77]

Addressing these limitations through meticulous experimental design and comprehensive analysis will enhance the robustness and reliability of future preclinical studies.

CONCLUSION

In conclusion, the use of DMR with LED/OLED catheters offers a promising non-pharmacological therapeutic approach for managing T2DM and associated liver conditions like non-alcoholic fatty liver disease approach to positively impact glycemic control, reduce insulin resistance, target pancreatic islet regeneration, and modulate the gut microbiome. These studies collectively suggest that DMR, particularly using advanced delivery methods including endoscopic DMR application, could offer a novel and effective approach to managing T2DM, with benefits extending to metabolic regulation and gut microbiome modulation.

The positive results from our studies demonstrated the potential benefits of these technologies in clinical applications, providing a foundation for further research to optimize and understand the mechanisms underlying these effects. Further research is needed to confirm these findings and explore the long-term implications and safety of such treatments in human clinical trials.

The advancements in DMR technology, particularly with the incorporation of dual wavelengths, suggest that these treatments could play a significant role in future diabetes management strategies, improving patient outcomes and offering a novel approach to addressing metabolic disorders.

REFERENCE

1.   Chatterjee S, Khunti K, Davies MJ: **Type 2 diabetes**. *Lancet* 2017, **389**(10085):2239-2251.

2.   Chamine I, Larson A, Huguet N, Angier H, Valenzuela S, Dinh D, Hwang J: **Characterizing acute and chronic complications among patients with diabetes mellitus in community health centers**. *Ann Fam Med* 2022, **20**(20 Suppl 1).

3.   **Diagnosis and classification of diabetes mellitus**. *Diabetes Care* 2014, **37 Suppl 1**:S81-90.

4.   Katsarou A, Gudbjörnsdottir S, Rawshani A, Dabelea D, Bonifacio E, Anderson BJ, Jacobsen LM, Schatz DA, Lernmark Å: **Type 1 diabetes mellitus**. *Nat Rev Dis Primers* 2017, **3**:17016.

5.   **Diagnosis and classification of diabetes mellitus**. *Diabetes Care* 2010, **33 Suppl 1**(Suppl 1):S62-69.

6.   DeFronzo RA, Ferrannini E, Groop L, Henry RR, Herman WH, Holst JJ, Hu FB, Kahn CR, Raz I, Shulman GI *et al*: **Type 2 diabetes mellitus**. *Nat Rev Dis Primers* 2015, **1**:15019.

7.   Sun H, Saeedi P, Karuranga S, Pinkepank M, Ogurtsova K, Duncan BB, Stein C, Basit A, Chan JCN, Mbanya JC *et al*: **IDF Diabetes Atlas: Global, regional and country-level diabetes prevalence estimates for 2021 and projections for 2045**. *Diabetes Research and Clinical Practice* 2022, **183**:109119.

8.   **Diabetes Fact Sheet in Korea 2022**. *Korean Diabetes Association* 2022.

9.   **9. Pharmacologic Approaches to Glycemic Treatment: Standards of Medical Care in Diabetes-2020**. *Diabetes Care* 2020, **43**(Suppl 1):S98-s110.

10.   Doyle-Delgado K, Chamberlain JJ, Shubrook JH, Skolnik N, Trujillo J: **Pharmacologic Approaches to Glycemic Treatment of Type 2 Diabetes: Synopsis of the 2020 American Diabetes Association's Standards of Medical Care in Diabetes Clinical Guideline**. *Ann Intern Med* 2020, **173**(10):813-821.

11.   Dardi I, Kouvatsos T, Jabbour SA: **SGLT2 inhibitors**. *Biochem Pharmacol* 2016,

101:27-39.

12. Carpio GR, Fonseca VA: **Update on Safety Issues Related to Antihyperglycemic Therapy**. *Diabetes Spectr* 2014, **27**(2):92-100.

13. Scheen AJ: **SGLT2 Inhibitors: Benefit/Risk Balance**. *Curr Diab Rep* 2016, **16**(10):92.

14. Kurosaki E, Ogasawara H: **Ipragliflozin and other sodium–glucose cotransporter-2 (SGLT2) inhibitors in the treatment of type 2 diabetes: Preclinical and clinical data**. *Pharmacology & Therapeutics* 2013, **139**(1):51-59.

15. Lim GE, Huang GJ, Flora N, LeRoith D, Rhodes CJ, Brubaker PL: **Insulin regulates glucagon-like peptide-1 secretion from the enteroendocrine L cell**. *Endocrinology* 2009, **150**(2):580-591.

16. Li S, Vandvik PO, Lytvyn L, Guyatt GH, Palmer SC, Rodriguez-Gutierrez R, Foroutan F, Agoritsas T, Siemieniuk RAC, Walsh M *et al*: **SGLT-2 inhibitors or GLP-1 receptor agonists for adults with type 2 diabetes: a clinical practice guideline**. *Bmj* 2021, **373**:n1091.

17. Hauber AB, Nguyen H, Posner J, Kalsekar I, Ruggles J: **A discrete-choice experiment to quantify patient preferences for frequency of glucagon-like peptide-1 receptor agonist injections in the treatment of type 2 diabetes**. *Curr Med Res Opin* 2016, **32**(2):251-262.

18. Hernandez I, Sullivan SD: **Net prices of new antiobesity medications**. *Obesity (Silver Spring)* 2024, **32**(3):472-475.

19. Caruso I, Di Gioia L, Di Molfetta S, Cignarelli A, Palmer SC, Natale P, Strippoli GFM, Perrini S, Natalicchio A, Laviola L *et al*: **Glucometabolic outcomes of GLP-1 receptor agonist-based therapies in patients with type 2 diabetes: a systematic review and network meta-analysis**. *EClinicalMedicine* 2023, **64**:102181.

20. Sun F, Chai S, Yu K, Quan X, Yang Z, Wu S, Zhang Y, Ji L, Wang J, Shi L: **Gastrointestinal adverse events of glucagon-like peptide-1 receptor agonists in patients with type 2 diabetes: a systematic review and network meta-analysis**. *Diabetes Technol Ther* 2015, **17**(1):35-42.

21. Mancini GBJ, O'Meara E, Zieroth S, Bernier M, Cheng AYY, Cherney DZI, Connelly

KA, Ezekowitz J, Goldenberg RM, Leiter LA *et al*: **2022 Canadian Cardiovascular Society Guideline for Use of GLP-1 Receptor Agonists and SGLT2 Inhibitors for Cardiorenal Risk Reduction in Adults**. *Can J Cardiol* 2022, **38**(8):1153-1167.

22. Artasensi A, Pedretti A, Vistoli G, Fumagalli L: **Type 2 Diabetes Mellitus: A Review of Multi-Target Drugs**. *Molecules* 2020, **25**(8).

23. Rosenstock J, Wysham C, Frías JP, Kaneko S, Lee CJ, Fernández Landó L, Mao H, Cui X, Karanikas CA, Thieu VT: **Efficacy and safety of a novel dual GIP and GLP-1 receptor agonist tirzepatide in patients with type 2 diabetes (SURPASS-1): a double-blind, randomised, phase 3 trial**. *Lancet* 2021, **398**(10295):143-155.

24. Kanbay M, Copur S, Siriopol D, Yildiz AB, Gaipov A, van Raalte DH, Tuttle KR: **Effect of tirzepatide on blood pressure and lipids: A meta-analysis of randomized controlled trials**. *Diabetes Obes Metab* 2023, **25**(12):3766-3778.

25. Coskun T, Sloop KW, Loghin C, Alsina-Fernandez J, Urva S, Bokvist KB, Cui X, Briere DA, Cabrera O, Roell WC *et al*: **LY3298176, a novel dual GIP and GLP-1 receptor agonist for the treatment of type 2 diabetes mellitus: From discovery to clinical proof of concept**. *Mol Metab* 2018, **18**:3-14.

26. Inzucchi SE, Bergenstal RM, Buse JB, Diamant M, Ferrannini E, Nauck M, Peters AL, Tsapas A, Wender R, Matthews DR: **Management of hyperglycemia in type 2 diabetes: a patient-centered approach: position statement of the American Diabetes Association (ADA) and the European Association for the Study of Diabetes (EASD)**. *Diabetes Care* 2012, **35**(6):1364-1379.

27. Russell-Jones D, Khan R: **Insulin-associated weight gain in diabetes--causes, effects and coping strategies**. *Diabetes Obes Metab* 2007, **9**(6):799-812.

28. West JA, Ghosh SS, Parkes DG, Tsakmaki A, Grønlund RV, Pedersen PJ, Maggs D, Rajagopalan H, Bewick GA: **Peptide-based GIP receptor inhibition exhibits modest metabolic changes in mice when administered either alone or combined with GLP-1 agonism**. *bioRxiv* 2020:822122.

29. Muto H, Honda T, Tanaka T, Yokoyama S, Yamamoto K, Ito T, Imai N, Ishizu Y, Maeda K, Ishikawa T *et al*: **Proteomic Analysis Reveals Changes in Tight Junctions in the Small Intestinal Epithelium of Mice Fed a High-Fat Diet**. *Nutrients* 2023,

15(6).

30.   Casselbrant A, Wallenius V, Elebring E, Marschall HU, Johansson BR, Helander HF, Fändriks L: **Morphological Adaptation in the Jejunal Mucosa after Iso-Caloric High-Fat versus High-Carbohydrate Diets in Healthy Volunteers: Data from a Randomized Crossover Study**. *Nutrients* 2022, **14**(19).

31.   Soares A, Beraldi EJ, Ferreira PE, Bazotte RB, Buttow NC: **Intestinal and neuronal myenteric adaptations in the small intestine induced by a high-fat diet in mice**. *BMC Gastroenterol* 2015, **15**:3.

32.   Gniuli D, Calcagno A, Dalla Libera L, Calvani R, Leccesi L, Caristo ME, Vettor R, Castagneto M, Ghirlanda G, Mingrone G: **High-fat feeding stimulates endocrine, glucose-dependent insulinotropic polypeptide (GIP)-expressing cell hyperplasia in the duodenum of Wistar rats**. *Diabetologia* 2010, **53**(10):2233-2240.

33.   van Baar ACG, Nieuwdorp M, Holleman F, Soeters MR, Groen AK, Bergman JJGHM: **The Duodenum harbors a Broad Untapped Therapeutic Potential**. *Gastroenterology* 2018, **154**(4):773-777.

34.   Nguyen NT, Varela JE: **Bariatric surgery for obesity and metabolic disorders: state of the art**. *Nature Reviews Gastroenterology & Hepatology* 2017, **14**(3):160-169.

35.   Scheen AJ, De Flines J, De Roover A, Paquot N: **Bariatric surgery in patients with type 2 diabetes: benefits, risks, indications and perspectives**. *Diabetes Metab* 2009, **35**(6 Pt 2):537-543.

36.   Bradley D, Magkos F, Klein S: **Effects of bariatric surgery on glucose homeostasis and type 2 diabetes**. *Gastroenterology* 2012, **143**(4):897-912.

37.   **Standards of medical care in diabetes--2014**. *Diabetes Care* 2014, **37 Suppl 1**:S14-80.

38.   Longo S, Rizza S, Federici M: **Microbiota-gut-brain axis: relationships among the vagus nerve, gut microbiota, obesity, and diabetes**. *Acta Diabetologica* 2023, **60**(8):1007-1017.

39.   van Baar ACG, Devière J, Hopkins D, Crenier L, Holleman F, Galvão Neto MP, Becerra P, Vignolo P, Rodriguez Grunert L, Mingrone G *et al*: **Durable metabolic improvements 2 years after duodenal mucosal resurfacing (DMR) in patients**

with type 2 diabetes (REVITA-1 Study). *Diabetes Research and Clinical Practice* 2022, **184**:109194.

40. Busch C, Meiring S, Van Baar A, Holleman F, Nieuwdorp M, Bergman J: **RE-CELLULARIZATION VIA ELECTROPORATION THERAPY (RECET) COMBINED WITH GLP-1RA TO REPLACE INSULIN THERAPY IN PATIENTS WITH TYPE 2 DIABETES 6 MONTHS RESULTS OF THE EMINENT STUDY**. *Gastrointestinal Endoscopy* 2023, **97**(6):AB298.

41. Sartoretto A, O'Neal D, Holt B, Napier-Flood F, Rattan A, Yuan CY, Cameron G, Marinos G, Dayyeh BA: **DUODENAL MUCOSAL REGENERATION INDUCED BY ENDOSCOPIC PULSED ELECTRIC FIELD TREATMENT IMPROVES GLYCEMIC CONTROL IN PATIENTS WITH TYPE II DIABETES - INTERIM RESULTS FROM A FIRST-IN-HUMAN STUDY**. *Gastrointestinal Endoscopy* 2023, **97**(6):AB1034-AB1035.

42. Freitas LFd, Hamblin MR: **Proposed Mechanisms of Photobiomodulation or Low-Level Light Therapy**. *IEEE Journal of Selected Topics in Quantum Electronics* 2016, **22**(3):348-364.

43. Kocherova I, Bryja A, Błochowiak K, Kaczmarek M, Stefańska K, Matys J, Grzech-Leśniak K, Dominiak M, Mozdziak P, Kempisty B *et al*: **Photobiomodulation with Red and Near-Infrared Light Improves Viability and Modulates Expression of Mesenchymal and Apoptotic-Related Markers in Human Gingival Fibroblasts**. *Materials (Basel)* 2021, **14**(12).

44. Hamblin MR, Nelson ST, Strahan JR: **Photobiomodulation and Cancer: What Is the Truth?** *Photomed Laser Surg* 2018, **36**(5):241-245.

45. Fekrazad R, Mirmoezzi A, Kalhori KA, Arany P: **The effect of red, green and blue lasers on healing of oral wounds in diabetic rats**. *J Photochem Photobiol B* 2015, **148**:242-245.

46. Tatmatsu-Rocha JC, de Castro CA, Sene-Fiorese M, Parizotto NA: **Light-emitting diode modulates carbohydrate metabolism by pancreatic duct regeneration**. *Lasers Med Sci* 2017, **32**(8):1747-1755.

47. Francisco CO, Beltrame T, Hughson RL, Milan-Mattos JC, Ferroli-Fabricio AM,

Galvão Benze B, Ferraresi C, Parizotto NA, Bagnato VS, Borghi-Silva A *et al*: **Effects of light-emitting diode therapy (LEDT) on cardiopulmonary and hemodynamic adjustments during aerobic exercise and glucose levels in patients with diabetes mellitus: A randomized, crossover, double-blind and placebo-controlled clinical trial**. *Complement Ther Med* 2019, **42**:178-183.

48.   Rahbar Layegh E, Fadaei Fathabadi F, Lotfinia M, Zare F, Mohammadi Tofigh A, Abrishami S, Piryaei A: **Photobiomodulation therapy improves the growth factor and cytokine secretory profile in human type 2 diabetic fibroblasts**. *J Photochem Photobiol B* 2020, **210**:111962.

49.   Silva G, Ferraresi C, de Almeida RT, Motta ML, Paixão T, Ottone VO, Fonseca IA, Oliveira MX, Rocha-Vieira E, Dias-Peixoto MF *et al*: **Insulin resistance is improved in high-fat fed mice by photobiomodulation therapy at 630 nm**. *J Biophotonics* 2020, **13**(3):e201960140.

50.   Tao L, Liu Q, Zhang F, Fu Y, Zhu X, Weng X, Han H, Huang Y, Suo Y, Chen L *et al*: **Microglia modulation with 1070-nm light attenuates Aβ burden and cognitive impairment in Alzheimer's disease mouse model**. *Light Sci Appl* 2021, **10**(1):179.

51.   Huang HH, Stillman TJ, Branham LA, Williams SC: **The Effects of Photobiomodulation Therapy on Porcine Islet Insulin Secretion**. *Photobiomodul Photomed Laser Surg* 2022, **40**(6):395-401.

52.   Bonifacio M, Benfato ID, de Almeida Cruz M, de Sales DC, Pandolfo IL, Quintana HT, Carvalho CPF, de Oliveira CAM, Renno ACM: **Effects of photobiomodulation on glucose homeostasis and morphometric parameters in pancreatic islets of diabetic mice**. *Lasers Med Sci* 2022, **37**(3):1799-1809.

53.   Liebman C, Loya S, Lawrence M, Bashoo N, Cho M: **Stimulatory responses in α- and β-cells by near-infrared (810 nm) photobiomodulation**. *J Biophotonics* 2022, **15**(3):e202100257.

54.   da Silva Tonetto L, da Silva CCF, Gonzatti N, Guex CG, Hartmann DD, Boschi ES, Lago PD, Trevisan ME, de Freitas Bauermann L, Jaenisch RB: **Effects of photobiomodulation on oxidative stress in rats with type 2 diabetes mellitus**. *Lasers Med Sci* 2023, **38**(1):90.

55. Antunes F, Boveris A, Cadenas E: **On the mechanism and biology of cytochrome oxidase inhibition by nitric oxide**. *Proc Natl Acad Sci U S A* 2004, **101**(48):16774-16779.

56. Hamid MA: **Low-level Laser Therapy on Postoperative Pain after Mandibular Third Molar Surgery**. *Ann Maxillofac Surg* 2017, **7**(2):207-216.

57. Koyama M, Wada R, Sakuraba H, Mizukami H, Yagihashi S: **Accelerated loss of islet beta cells in sucrose-fed Goto-Kakizaki rats, a genetic model of non-insulin-dependent diabetes mellitus**. *Am J Pathol* 1998, **153**(2):537-545.

58. Portha B, Giroix MH, Tourrel-Cuzin C, Le-Stunff H, Movassat J: **The GK rat: a prototype for the study of non-overweight type 2 diabetes**. *Methods Mol Biol* 2012, **933**:125-159.

59. Xi S, Yin W, Wang Z, Kusunoki M, Lian X, Koike T, Fan J, Zhang Q: **A minipig model of high-fat/high-sucrose diet-induced diabetes and atherosclerosis**. *Int J Exp Pathol* 2004, **85**(4):223-231.

60. Joo J, Choi GM, Lee C, Eom YS, Kye IS, Jang KS, Hwang ST, Kim JD, Choi KS: **Mini LED array transferred onto a flexible substrate using Simultaneous Transfer and Bonding (SITRAB) process and Anisotropic Solder Film (ASF)**. In: *2022 IEEE 72nd Electronic Components and Technology Conference (ECTC): 31 May-3 June 2022 2022*; 2022: 619-624.

61. Briese E: **Normal body temperature of rats: the setpoint controversy**. *Neurosci Biobehav Rev* 1998, **22**(3):427-436.

62. Gutch M, Kumar S, Razi SM, Gupta KK, Gupta A: **Assessment of insulin sensitivity/resistance**. *Indian J Endocrinol Metab* 2015, **19**(1):160-164.

63. Vdoviaková K, Petrovová E, Maloveská M, Krešáková L, Teleky J, Elias MZ, Petrášová D: **Surgical Anatomy of the Gastrointestinal Tract and Its Vasculature in the Laboratory Rat**. *Gastroenterol Res Pract* 2016, **2016**:2632368.

64. Varum FJ, Veiga F, Sousa JS, Basit AW: **An investigation into the role of mucus thickness on mucoadhesion in the gastrointestinal tract of pig**. *Eur J Pharm Sci* 2010, **40**(4):335-341.

65. Bicknell B, Liebert A, Johnstone D, Kiat H: **Photobiomodulation of the microbiome:**

implications for metabolic and inflammatory diseases. *Lasers Med Sci* 2019, **34**(2):317-327.

66. Yang JY, Lee YS, Kim Y, Lee SH, Ryu S, Fukuda S, Hase K, Yang CS, Lim HS, Kim MS *et al*: **Gut commensal Bacteroides acidifaciens prevents obesity and improves insulin sensitivity in mice**. *Mucosal Immunol* 2017, **10**(1):104-116.

67. Kang X, Zhan L, Lu X, Song J, Zhong Y, Wang Y, Yang Y, Fan Z, Jiang X, Sun R: **Characteristics of Gastric Microbiota in GK Rats with Spontaneous Diabetes: A Comparative Study**. *Diabetes Metab Syndr Obes* 2020, **13**:1435-1447.

68. Smith Byron J, Miller Richard A, Schmidt Thomas M: **Muribaculaceae Genomes Assembled from Metagenomes Suggest Genetic Drivers of Differential Response to Acarbose Treatment in Mice**. *mSphere* 2021, **6**(6):e00851-00821.

69. Labbé A, Ganopolsky JG, Martoni CJ, Prakash S, Jones ML: **Bacterial Bile Metabolising Gene Abundance in Crohn's, Ulcerative Colitis and Type 2 Diabetes Metagenomes**. *PLOS ONE* 2014, **9**(12):e115175.

70. Kaakoush NO: **Insights into the Role of Erysipelotrichaceae in the Human Host**. *Front Cell Infect Microbiol* 2015, **5**:84.

71. Dufrane D, van Steenberghe M, Guiot Y, Goebbels RM, Saliez A, Gianello P: **Streptozotocin-induced diabetes in large animals (pigs/primates): role of GLUT2 transporter and beta-cell plasticity**. *Transplantation* 2006, **81**(1):36-45.

72. Tu C-F, Hsu C-Y, Lee M-H, Jiang B-H, Guo S-F, Lin C-C, Yang T-S: **Growing pigs developed different types of diabetes induced by streptozotocin depending on their transcription factor 7-like 2 gene polymorphisms**. *Laboratory Animal Research* 2018, **34**(4):185-194.

73. Festing MF: **Design and statistical methods in studies using animal models of development**. *Ilar j* 2006, **47**(1):5-14.

74. Lagerwaard FJ, Verstegen NE, Haasbeek CJ, Slotman BJ, Paul MA, Smit EF, Senan S: **Outcomes of stereotactic ablative radiotherapy in patients with potentially operable stage I non-small cell lung cancer**. *Int J Radiat Oncol Biol Phys* 2012, **83**(1):348-353.

75. Kilkenny C, Browne WJ, Cuthill IC, Emerson M, Altman DG: **Improving bioscience**

research reporting: the ARRIVE guidelines for reporting animal research. *PLoS Biol* 2010, **8**(6):e1000412.

76.   Lazic SE: **The problem of pseudoreplication in neuroscientific studies: is it affecting your analysis?** *BMC Neurosci* 2010, **11**:5.

77.   Festing MF, Altman DG: **Guidelines for the design and statistical analysis of experiments using laboratory animals**. *Ilar j* 2002, **43**(4):244-258.

초록

1. 서론

　　제 2 형 당뇨병은 서구식 식습관과 고령화 인구 증가로 인해 만성 대사 질환 문제로 거론되고 있다. 제 2 형 당뇨병 치료에 대한 수요가 증가하고 있음에도 불구하고 약물만으로 혈당을 조절하는 것은 여전히 어려운 실정이다. 이에 혁신적인 비약물 치료법에 대한 연구 필요성이 제기되고 있다. 최근 십이지장이 대사 질환의 비약물 치료의 중요한 부위로 언급되고 있으며, 두꺼워진 점막을 표적하여 건강한 조직으로 재생시키는 십이지장 점막 재생이 연구되고 있다. 현재 십이지장 점막 재생 시술 방법은 복잡하고 비가역적 손상의 위험이 있어, 보다 안전하고 효과적인 비약물 치료 기기의 개발이 필요하다. 본 연구에서는 제 2 형 당뇨 질환 소동물 및 대동물 모델에서 새로이 고안된 십이지장 점막 재생 어플리케이션의 치료 효능과 안전성을 평가하며, 또한 십이지장 점막 재생 실험군과 대조군 간의 분자 생물학적 차이와 장내 미생물 변화를 정량 분석을 통해 치료 기전을 확인하고자 한다.

3. 연구 방법

　　본 연구에서는 제 2 형 당뇨 질환 Goto-Kakizaki (GK) 랫드 모델을 사용하여 카테터 형태의 light emitting diode (LED) / organic light emitting diode (OLED)를 이용한 십이지장 점막 재생 효과를 평가한다. LED 카테터를 이용한 실험에서는 이중 파장 (630/850 nm)과 단일 파장(630nm, 850nm)의 효능 차이를 확인하고, OLED 카테터를 이용한 실험에서는 면광원인 OLED 단일 파장 카테터의 안전성 및 치료 효능을 평가한다. 또한 임상 시험 진입을 위하여 제 2 형 질환 대동물 모델에 내시경 부착형 이중 파장의 LED 어플리케이션을 적용하여 안전성과 치료 효능을 평가한다. 제 2 형 당뇨 질환 모델 GK 랫드와 미니피그에서 경구 당 부하 시험을 수행하여 십이지장 점막 재생 후 관찰 동안 혈당 조절 능력을 관찰 및 평가한다. 혈장 샘플에서 간 기능 검사를 위한 생화학 분석을 진행하고, 효소면역분석법을 이용하여 인슐린, GLP-1, GIP 등 호르몬 분석을 수행한다. 십이지장, 간 및 췌장의 조직학적 검사는 일반 조직 염색 및 다중 면역 조직 화학 염색을 수행하여 조직 변화 및 췌장 소도 세포 및 조직 변화 형태 등을 정량적으로 평가한다. 십이지장 점막 재생 후 장내 마이크로바이옴의 변화를 확인하기 위해, 대조군 실험군의 관찰 기간에 따른 장내 미생물 군 조성 변화를 평가한다.

울산대학교
UNIVERSITY OF ULSAN

3. 연구 결과

본 연구를 통해 LED 및 OLED 카테터를 이용한 십이지장 빛 자극이 십이지장 점막 재생 및 제 2 형 당뇨병 관련 합병증 치료에 효과가 있음을 확인하였다. 본 연구는 제 2 형 당뇨 질환 동물 모델에서 적색 적외선의 이중파장 LED 소자의 카테터를 이용한 십이지장 점막 재생을 통해 혈당 조절 능력 및 간 기능 수치가 개선됨과 동시에 췌장 소도 세포 효율이 높아짐을 확인하였다. 유사하게, 적색의 OLED 소자의 카테터를 이용한 십이지장 점막 자극 후 질환 모델의 혈당 조절 능력 및 인슐린 저항성 개선을 확인하였다. LED/OLED 카테터를 이용한 십이지장 점막 자극은 간 섬유화를 지연시키고 장내 미생물 군집이 변화되었다. 또한 십이지장 점막 재생술 시행 후 제 2 형 당뇨질환 미니피그 모델에서도 혈당 조절 능력이 개선되고 공복 혈당이 유의미하게 감소하는 것을 확인하였다.

4. 결론

결론적으로, LED/OLED 카테터형 십이지장 점막 재생 시술 후 제 2 형 당뇨 발현 GK 랫드의 혈당 조절 능력을 개선하였고, 인슐린 저항성을 감소시키며, 췌장 소도 세포 재생, 장내 미생물 군집 변화를 유도하는 것을 확인하였다. 뿐만 아니라, 제 2 형 당뇨 유발 미니피그 모델에 적용한 내시경 부착형 LED 어플리케이션을 통해 십이지장 점막 자극 어플리케이션의 기능 구현뿐만 아니라, 질환 모델의 혈당 조절 능력 개선 또한 확인할 수 있었다. 이 연구 결과는 십이지장 점막 재생이 제 2 형 당뇨병을 포함한 대사 질환에 대한 효과적인 치료 방식으로 작용할 수 있음을 시사하며, 추후 이중 파장 LED 기반의 내시경 부착형 LED 어플리케이션을 적용한 임상 시험을 통해 새로운 비약물 치료 잠재력을 뒷받침할 수 있는 연구를 기대할 수 있다.

울산대학교
UNIVERSITY OF ULSAN